Amino Acids (2011) 41:363–385
DOI 10.1007/s00726-010-0649-5

ORIGINAL ARTICLE

Proteome analysis of microtubule-associated proteins and their interacting partners from mammalian brain

Frank Kozielski · Tahira Riaz · Salvatore DeBonis · Christian J. Koehler · Mario Kroening · Isabel Panse · Margarita Strozynski · Ian M. Donaldson · Bernd Thiede

Received: 26 February 2010 / Accepted: 1 June 2010 / Published online: 22 June 2010

Abstract The microtubule (MT) cytoskeleton is essential for a variety of cellular processes. MTs are finely regulated by distinct classes of MT-associated proteins (MAPs), which themselves bind to and are regulated by a large number of additional proteins. We have carried out proteome analyses of tubulin-rich and tubulin-depleted MAPs and their interacting partners isolated from bovine brain. In total, 573 proteins were identified giving us unprecedented access to brain-specific MT-associated proteins from mammalian brain. Most of the standard MAPs were identified and at least 500 proteins have been reported as being associated with MTs. We identified protein complexes with a large number of subunits such as brain-specific motor/adaptor/cargo complexes for kinesins, dynein, and dynactin, and proteins of an RNA-transporting granule. About 25% of the identified proteins were also found in the synaptic vesicle proteome. Analysis of the MS/MS data revealed many posttranslational modifications, amino acid changes, and alternative splice variants, particularly in tau, a key protein implicated in Alzheimer's disease. Bioinformatic analysis of known protein–protein interactions of the identified proteins indicated that the number of MAPs and their associated proteins is larger than previously anticipated and that our database will be a useful resource to identify novel binding partners.

Keywords Alternative splice variants · Brain · MAPs · Posttranslational modifications · Protein–protein interactions

Abbreviations

AMPPCP	Adenylyl 5′-(β,γ-methylene)diphosphonate
ATP	Adenosine triphosphate
EDTA	Ethylenediaminetetraacetic acid
GTP	Guanosine triphosphate
KLC	Kinesin light chain
MAPs	Microtubule-associated proteins
MgcRacGAP	Rac GTPase-activating protein 1
MKLP-1	Mitotic kinesin-like protein 1
MTs	Microtubules
PIPES	1,4-Piperazinediethanesulfonic acid
PMSF	Phenylmethanesulfonylfluoride
SVP	Synaptic vesicle protein
TAME	N_α-*p*-Tosyl-L-arginine methyl ester

Introduction

Microtubules (MTs) are highly regulated and integral components of the cellular cytoskeleton (Dutcher 2001;

Electronic supplementary material The online version of this article (doi:10.1007/s00726-010-0649-5) contains supplementary material, which is available to authorized users.

F. Kozielski
The Beatson Institute for Cancer Research, Switchback Road, Bearsden, Glasgow G61 1BD, Scotland, UK

T. Riaz · C. J. Koehler · M. Kroening · I. Panse · M. Strozynski · I. M. Donaldson · B. Thiede
The Biotechnology Centre of Oslo, University of Oslo, Gaustadalleen 21, 0349 Oslo, Norway

S. DeBonis
Institut de Biologie Structurale (CEA-CNRS-UJF), 41 rue Jules Horowitz, 38027 Grenoble Cedex 01, France

B. Thiede (✉)
The Biotechnology Centre of Oslo, University of Oslo, Gaustadalleen 21, P.O. Box 1125, Blindern, 0317 Oslo, Norway
e-mail: bernd.thiede@biotek.uio.no

McKean et al. 2001). They are not only key players during cell division, in particular mitosis and cytokinesis (Sharp et al. 2000), but have also a large number of non-mitotic cellular functions. MTs are composed of α/β-tubulin heterodimers, which assemble into MTs by forming linear protofilaments (Wade 2007). MTs have distinct polarity and can be composed of 9–13 parallel protofilaments. Furthermore, MTs are in a dynamic equilibrium with the intracellular tubulin pool and are influenced by guanosine triphosphate (GTP), the ionic environment, and a large family of proteins called microtubule-associated proteins (MAPs) that regulate their dynamics (Amos and Schlieper 2005; Maiato et al. 2004).

MT assembly and disassembly within the cell is controlled by a balance between MT-stabilizing and destabilizing proteins. Stabilizing proteins include MAP1, MAP2, MAP4, and tau. Phosphorylation of these proteins by protein kinases including $p34^{cdc2}$ increases during mitosis reducing their affinity for MTs and thus their ability to promote polymerization. Destabilizing proteins include stathmin (Oncoprotein 18, Op18), katanin, and certain members of the kinesin-13 family (KIF2's), which are known MT-depolymerisers. Phosphorylation of stathmin by $p34^{cdc2}$ increases the MT catastrophy rate during mitosis. Furthermore, the two major classes of MT-dependent motor proteins, kinesins (Hirokawa and Noda 2008) and dyneins (Hook and Vallee 2006), are critical for MT function. They bind to MTs and use the energy derived from ATP hydrolysis to transport cargo either to the plus- or minus-end of MTs, respectively. Moreover, the identification of molecules involved in signaling pathways (e.g., Hedgehog, Wnt, JNK kinase, and ERK kinase) that interact with MTs indicates their importance in certain signaling transduction pathways (Gundersen and Cook 1999; Mollinedo and Gajate 2003; Moss and Lane 2006).

Compounds that interfere with MT dynamics are among the most successful and widely used chemotherapeutic drugs (Jordan and Wilson 2004). Disruption of MT dynamics by MT-targeting drugs, such as vinca alkaloids and taxanes, leads to mitotic arrest and subsequently to apoptosis. However, these drugs have severe drawbacks such as the development of resistance, caused for example by drug removal by membrane pumps, such as P-glycoprotein (Ambudkar et al. 2003), or by overexpression of different tubulin isoforms or point mutations (Kavallaris et al. 2001). Not surprisingly, several MAPs have themselves become potential targets for cancer chemotherapy (Bhat and Setaluri 2007).

The organization of MTs in neurons differs in several ways from non-neuronal cells. Brain MTs contain tubulin of many different isotypes, with a variety of posttranslational modifications and a large number of MAPs. For example, class III and IVa β-tubulins are neuron-specific and posttranslational modifications of α-tubulin (carboxy-terminal detyrosination and lysine ε-acetylation) and β-tubulin (polyglutamylation of a glutamate residue near the carboxy-terminus) have been identified in brain. MAP1 and MAP2 are expressed primarily in neurons; MAP4 is ubiquitously expressed, and MAP7 is restricted to epithelial cells. Tau is found mainly in neurons, where its phosphorylated isoforms bind to tubulin to promote polymerization and stabilization of axonal MTs. Abnormal phosphorylation of tau is associated with neurodegenerative disorders such as Alzheimer's disease (Wang et al. 2007).

The MT-associated proteome has been investigated in three different species: 45 potential MAPs have been identified in *Xenopus laevis* and 21 of these were previously shown to interact with MTs (Gache et al. 2007; Liska et al. 2004). Very recently, 318 MAPs of *Xenopus* egg extracts were identified to build-up the meiotic MAPs interactome (Gache et al. 2010). In *Arabidopsis thaliana*, 122 MAPs were identified, including 52 with a known interaction with tubulin or MTs (Chuong et al. 2004). Recently, 270 MAPs and their associated proteins have been found in *Drosophila melanogaster* embryos, identifying many complexes with mitotic functions (Hughes et al. 2008).

Mammalian brain tissue is easily accessible and many MAPs have been identified and studied using bovine brain. We wanted to establish a MAP proteome of mammalian brain since the increased life span in many industrial countries is accompanied by a growing importance of neurodegenerative diseases, several of which are likely to be associated with the MT network. In the work presented here, we established the first proteome databases of MAPs isolated from mammalian brain, using two distinct biochemical preparations named "tubulin-rich" and "tubulin-depleted". In total, we identified 573 proteins that potentially interact either directly or indirectly with MTs. Of these at least 500 are known to be associated with MTs. We have identified for the first time a number of brain-specific proteins, 80% of which are known to interact with MTs or MAPs. In addition to the many MAPs, we also found a large number of MAP-associated proteins that indirectly bind to MTs by forming complexes with the MAPs. Finally, we identified a large number of posttranslational modifications, amino acid changes, and alternative splice variants of several MAPs indicating their complex regulation.

Materials and methods

Preparation of tubulin-rich MAPs

ATP, AMP-PCP, PIPES, EDTA, PMSF, taxol, and sucrose were purchased from Sigma. A fresh brain, obtained from

the slaughter house, of an animal younger than 18 months was placed into ice-cooled buffer A (50 mM PIPES, pH 7, 2 mM $MgCl_2$, 1 mM EDTA, 1 mM PMSF, 10 μg/ml, leupeptin, 10 μg/ml TAME, 10 μg/ml benzamidine, 10 μg/ml aprotinin) and mixed three times for 30 s in a precooled Waring blender. The homogenate was centrifuged at 4°C for 30 min at 12,000 rpm (Beckman J2-21, rotor JA-14) and the pellet was discarded. The supernatant was further centrifuged at 45,000 rpm in a Beckman L80 ultracentrifuge (Ti 45 rotor) at 4°C for 60 min. The resulting pellet was discarded, and 20 μM taxol, 3 μM $MgCl_2$, and 3 mM AMP-PCP were added to the supernatant (S1-AMP-PCP). We then incubated the supernatant for 30 min at 37°C to promote MT polymerisation. The MAP-rich taxol-stabilized MTs were centrifuged at 18,000 rpm (Beckman J2-21, JA-20 rotor) at 37°C on a cushion of 7.5% sucrose in buffer A. The resulting pellet (P2-AMP-PCP) was further washed with 2 ml buffer A, supplemented with AMP-PCP, and centrifuged for 30 min at 18,000 rpm (Beckman J2-21, JA-20 rotor). The resulting pellet containing MAP-rich MTs purified in the presence of AMP-PCP (P3-AMP-PCP) as well as the corresponding supernatant (S3-AMP-PCP) was frozen in liquid nitrogen until used for proteome analysis.

Preparation of tubulin-depleted MAPs

A fresh brain from a slaughtered animal was cleaned from blood clots, placed into 150 ml ice-cooled MEM buffer (100 mM MES, pH 6.75, 1 mM EGTA, 1 mM $MgCl_2$) and mixed 3 times for 30 s in a Waring blender. The mixture was centrifuged at 4°C for 45 min at 13,500 rpm (Beckman J2-21, rotor JA-14) and the pellet was discarded. The supernatant was transferred to an ultracentrifuge and centrifuged for 30 min at 35,000 rpm (Beckman L80 ultracentrifuge, Ti-45 rotor). The resulting supernatant was supplemented with 2 mM Mg^{2+}ATP and 20% (v/v) glycerol and incubated for 40 min at 37°C to allow the polymerisation of tubulin into MTs. MTs with associated MAPs were pelleted at 37°C on a glycerol cushion (30 ml) for 60 min at 40,000 rpm (Beckman L80 ultracentrifuge Ti-45). The supernatant was discarded and the pellet was placed on ice for 10 min to allow the depolymerisation of MTs. The mixture was then transferred to a glass tissue grinder and carefully homogenised in MEM buffer to depolymerise the remaining MTs into tubulin. The supernatant was applied onto a self-packed phosphocellulose column (300 ml phosphocellulose P11 Whatman). In this procedure, tubulin was captured in the flow-through, whereas MAPs are retained on the column material (Williams and Lee 1982). The column was further washed with MEM buffer until the absorbance at 280 nm reached zero. Finally, MAPs bound to the column were eluted by applying MEM buffer supplemented with 3 M NaCl. The eluate was aliquoted, frozen in liquid nitrogen, and stored at −80°C until used for proteome analysis.

Gel electrophoresis

SDS-PAGE was performed with 4% stacking gel and 10% separation gel using a Multigel-long gel system (BioSite, Täby, Sweden) (Laemmli 1970). Gels were stained with Coomassie Brilliant Blue G-250 (Serva, Heidelberg, Germany) employing the blue silver staining technique with slight modifications (Candiano et al. 2004). Fixation was performed with 50% ethanol/2% phosphoric acid for 1 h, incubation with 34% ethanol/2% phosphoric acid/17% ammonium sulfate for 1 h, and staining with 20% methanol/10% phosphoric acid/10% ammonium sulfate for 1 h. Finally, the gels were washed once for 30 min with 25% ethanol and three times with water.

Mass spectrometry

The Coomassie Brilliant Blue G-250 stained gel lanes were excised into 24 bands for in-gel digestion with 0.1 μg trypsin (Promega, Madison, WI, USA) in 20 μl 25 mM ammonium bicarbonate, pH 7.8 at 37°C for 16 h. For each band the tryptic peptides were purified with μ-C18 ZipTips (Millipore, Billerica, MA, USA), and dried using a Speed Vac concentrator (Savant, Holbrook, NY, USA). The dried peptides were dissolved in 10 μl 1% formic acid in water and 5 μl was injected onto an LC/MS system consisting of a 1200 series liquid chromatograph, HPLC-Chip Cube MS interface, and a 6330 LC/MSD Trap XCT Ultra ion trap mass spectrometer (Agilent Technologies, Waldbronn, Germany). The system was equipped with an HPLC Chip (Agilent Technologies, Waldbronn, Germany) that incorporated a 40-nl enrichment column and a 43 mm × 75 μm analytical column packed with 5 μm Zorbax 300SB-C18 particles. Peptides were loaded onto the enrichment column with 97% solvent A (water with 0.1% formic acid) and 3% B (90% acetonitrile with 0.1% formic acid) at 4 μl/min. They were then eluted with a gradient from 3% B to 55% B in 30 min, followed by a steep gradient to 80% B in 1 min at a flow rate of 300 nl/min. The total runtime, including column reconditioning, was 43 min. Molecular masses were recorded using data-dependent MS/MS acquisition. The MS and MS/MS conditions employed were as follows: Drying gas flow: 4 l/min; drying temperature: 300°C; capillary voltage: 1,900 V; skim 1: 40 V; capillary exit: 158.5 V; trap drive: 84.3; averages: 1; ion current control: on; maximum accumulation time: 150 ms; smart target: 450,000; MS scan range: 300–2,000; standard-enhanced: on. MS/MS: number of parents: 5; fragmentation amplitude: 1.30 V; SmartFrag: on, 30–200%; active exclusion:

on, 2 spectra, 1 min; exclude +1: on, MS/MS scan range: 100–2,000; ultra scan: on; ion current control target: 450,000. MS scan events and HPLC solvent gradient were controlled by DataAnalysis version 3.4. Compound detection was performed with the following parameters: S/N threshold: 5, area threshold: 10%, intensity threshold: 10%, smoothing width: 1, spectrum type: auto, background subtraction: none, intensity threshold 10,000, maximum number of compounds: 500, retention time window: 0.5 min. The compounds were exported for each LC run as mgf files.

Protein identification

The SwissProt database (15.01.2008) with 11,256 sequences for "other mammalian" and 18,117 sequences for "homo sapiens" was searched using the Mascot in-house version 2.2 (Perkins et al. 1999). A tolerance of *m/z* 0.5 was allowed for the precursor mass and MS/MS fragments. Furthermore, trypsin was selected as enzyme considering up to two missed cleavage sites, peptide charge 2+ and 3+, and variable protein modifications were allowed, such as oxidation (met), *N*-acetyl (protein), propionamide (cys), and pyro-glu (N-term Q). Automatic decoy database searches were performed in Mascot and revealed a false discovery rate for peptide matches above an identity threshold of less than 2%. Proteins were considered to be identified if at least two tryptic peptides with an individual ion score of at least 20 were found with a total Mascot score of at least 50 (MudPit scoring protein threshold 35–41). "Show subsets" and "require bold red" were applied on initial Mascot search results to eliminate redundancy. For automatic error-tolerant searches of uninterpreted MS/MS data, the same parameters were used with the exception that only one missed cleavage site for trypsin, oxidation (met), and *N*-acetyl (protein) were allowed (Perkins et al. 1999). Post-translational modifications were assigned by Mascot and manually evaluated. The mgf files and dat files of searches in SwissProt/human were uploaded into the Proteomics Identification database (PRIDE) using the PRIDE converter (Barsnes et al. 2009) and are available at http://www.ebi.ac.uk/pride/ with accession numbers 12173–12187.

Error-tolerant search to identify posttranslational modifications and amino acid exchanges

To identify posttranslational modifications and amino acid exchanges, the MS/MS datasets with the highest number of proteins and Mascot score of tubulin-rich and tubulin-depleted MAPs were searched in Swiss-Prot against bovine sequences using the automatic error-tolerant search function in Mascot. Thereby, proteins identified with scores above the homology threshold were selected for an error-tolerant second pass search to order unmatched MS/MS spectra to these proteins. Only one of the following rules was allowed for one peptide: (i) trypsin as selected enzyme became semi-specific, (ii) the complete list of modifications according to Unimod was checked, and (iii) amino acid substitutions that arise from single base substitutions were tested. The ion score cut-off was set to 30.

The additional peptide matches were checked after the following error-tolerant search. Because of well-known modifications artificially generated by sample treatment and gel electrophoresis, the following mass changes were excluded: +1 Da for deamidation of asparagines and glutamines, +16 Da for methionine- and tryptophan-containing peptides (oxidation), +32 Da for at least two methionine-containing peptides (oxidation), +71 Da for cysteine-containing peptides (cysteine alkylation to propionamide), and −17 Da for peptides with N-terminal glutamine (pyroglutamylation). In addition, +28 Da was excluded for aspartic acid and glutamic acid-containing peptides due to our gel staining conditions. Moreover, we observed several cysteine-containing peptides with a mass shift of +76 Da, most likely due to the modification by β-mercaptoethanol. Mass shifts of +128 Da and +156 Da were excluded if the peptide contained a lysine or arginine, respectively, following the cleavage site. Furthermore, combinations of these artificial modifications were observed such as +17 Da (methionine oxidation and deamidation of asparagines and glutamine) +72 Da (cysteine alkylation to propionamide and deamidation of asparagine and glutamine), and +87 Da (cysteine alkylation to propionamide and methionine oxidation). Moreover, large mass differences (>400 Da) were usually obtained due to wrong calculation of 3+ ions as 2+ charged. Biological modifications and amino acid substitutions according to Unimod (http://www.unimod.org/modifications_list.php) were compared with the potential and predicted amino acid positions according to Mascot and MS/MS fragmentation pattern.

Identification of alternative splice variants

A Fasta database of "other mammalia" was generated using the "varsplic" perl script (ftp://ftp.ebi.ac.uk/pub/software/swissprot/varsplic/) and the supporting module "Swissknife" (ftp://ftp.ebi.ac.uk/pub/software/swissprot/Swissknife/) from EBI (Hermjakob et al. 1999) that generates additional sequences representing the splice isoforms, variants and conflicts described in Swiss-Prot annotations. Again, the datasets with the highest number of proteins and Mascot scores of tubulin-rich and tubulin-depleted MAPs were searched against this database. Proteins with the same entry number, which were identified at least twice, were evaluated to find sequence-specific peptides derived from alternative splice variants.

Phosphopeptide isolation using TiO_2 beads

SDS-PAGE lanes of tubulin-rich and tubulin-depleted MAPs were cut into six equal pieces and digested with trypsin. The peptides were purified using μ-C18 ZipTips, dissolved in 50 µl 0.1% trifluoroacetic acid, and 0.25 mg Titansphere TiO_2 beads suspended in 10 µl acetonitrile were added for 10 min at room temperature to bind phosphopeptides (a generous gift of Dr. Andreas Schlosser, Charite Berlin, Germany). The supernatant was discarded after centrifugation and the beads were washed with 100 µl 100 mM ammonium glutamate to increase the efficiency of phosphopeptide enrichment (Yu et al. 2007). The peptides were eluted from the TiO_2 beads with 2×50 µl 1% ammonium hydroxide. Subsequently, 8 µl 25% formic acid was added to the eluted peptides. Finally, the peptides were purified using μ-C18 ZipTips before analysis by LC–MS/MS.

Protein–protein interaction map

UniProtIDs from Supplementary table 9 (e.g., DHYC_HUMAN) were converted to their corresponding UniProt Accessions (e.g., Q14204) using UniProt's ID Mapping Service (http://www.uniprot.org and Razick et al. (2008)). These were used to search release 2.0 of the iRefIndex using the Cytoscape plugin (see (2008) and http://irefindex.uio.no). This release of iRefIndex includes data from nine interaction databases including BIND (Alfarano et al. 2005; Bader et al. 2003), BioGRID (Stark et al. 2006), DIP (Salwinski et al. 2004), HPRD (Mishra et al. 2006; Peri et al. 2003), IntAct (Hermjakob et al. 2004; Kerrien et al. 2007), MINT (Chatr-aryamontri et al. 2007), MPact (Guldener et al. 2006), MPPI (Pagel et al. 2005), and OPHID (Brown and Jurisica 2005). Figure 5 was constructed using version 2.6.1 of Cytoscape (see Shannon et al. 2003 and http://cytoscape.org).

Results

Identification of tubulin-rich MAPs from bovine brain

Tubulin-rich MAPs from bovine brain were prepared by in situ taxol-enhanced tubulin polymerization and purified by centrifugation. Three replicates of the MAP-MT pellet were separated by SDS-PAGE (Fig. 1a). Gel lanes were cut into 24 bands, digested with trypsin, and analyzed by nanoLC-MS/MS using a ChipLC-ion trap electrospray mass spectrometer. Subsequently, the Mascot search engine was applied to analyze the mass spectrometry data. The first dataset was searched against Swiss-Prot using "other mammalia" with 16,521 sequences and revealed 281 bovine proteins with $p < 0.05$ (Supplementary table 1). However, searching the same dataset against "human" in Swiss-Prot (18,117 sequences) identified 370 proteins with $p < 0.05$ (Supplementary table 2). Considering the entry names, 202 identical proteins were identified in "bovin" and "human", 168 unique proteins were found in human, and 79 proteins were identified exclusively in bovine (Fig. 2a and Supplementary table 3). Subsequently, the database of tubulin-rich MAPs was built-up using human sequences. The full search of three biological replicates against Swiss-Prot using human sequences revealed 353 different proteins with a protein score of at least 50 and at least two matched queries (Supplementary table 4).

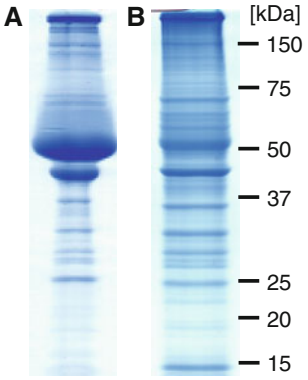

Fig. 1 SDS-PAGE of tubulin-rich and tubulin-depleted MAPs. The Coomassie G-250 stained gel lanes of tubulin-rich (**a**) and tubulin-depleted (**b**) MAPs are shown. The intense tubulin band in the tubulin-rich preparation at 50 kDa was significantly reduced after depletion (**b**)

Identification of tubulin-depleted MAPs from bovine brain

Coomassie G-250 stained SDS-PAGE showed that more than 80% of the total protein amount consisted of α/β-tubulin using the preparation of MAPs by taxol-enhanced tubulin polymerization (Fig. 1a). To obtain access to less abundant proteins and to investigate whether the biochemical purification procedure plays a role in identifying MAPs, tubulins were separated from MAPs by using a phosphocellulose-based column. Thereby, the amount of tubulins was significantly reduced when comparing the Coomassie G-250 stained SDS-PAGE gels of tubulin-rich (Fig. 1a) with tubulin-depleted (Fig. 1b) MAPs. Tubulin-depleted MAPs were identified with the same approach as applied to tubulin-rich MAPs using trypsin digestion of the SDS-PAGE lanes, nanoLC-MS/MS and data searches employing Mascot. Again, the Mascot search with one dataset against "other mammalia" identified less proteins (Supplementary table 5) as against the human database (Supplementary table 6) with 366 and 473 proteins,

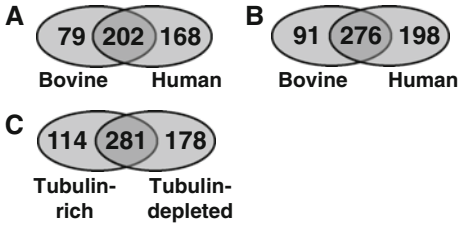

Fig. 2 Identification of tubulin-rich and tubulin-depleted MAPs searched in bovine and human. The number of proteins identified with the same dataset in bovine and human are displayed for tubulin-rich (**a**) and tubulin-depleted MAPs (**b**). More proteins were identified in human than in bovine (**a** and **b**). 573 unique proteins were identified searching the MS data in human for both preparations of MAPs (**c**). A higher number of proteins were identified in the tubulin-depleted (178) compared to the tubulin-rich (114) preparation (**c**)

respectively ($p < 0.05$). Based on the entry names, 276 identical proteins were identified in "bovin" and "human", 198 unique proteins were found in human, and 91 proteins were identified only in bovine (Fig. 2b and Supplementary table 7). Eventually, the database of tubulin-depleted MAPs was constructed using human sequences. The search of three biological replicates against Swiss-Prot in human sequences revealed 429 different proteins with a protein score of at least 50 and two matched queries (Supplementary table 8).

Comparison of tubulin-rich and tubulin-depleted MAPs from bovine brain

The depletion of tubulins has increased the number of identified proteins from 353 to 429. The combined databases of tubulin-rich and tubulin-depleted MAPs included 573 proteins with 281 in common, 114 unique proteins in tubulin-rich MAPs, and 178 unique proteins derived from tubulin-depleted MAPs (Fig. 2c, and Supplementary table 9). Echinoderm MT-associated protein-like (1, 2, 3, and 4), several kinesins and their associated light-chains (KIF5A, KIF5B, KLC1, KLC2, and KLC4, KIF21A, KIF23), myosins (Myosin-10, 9, Va, and VI), Ras-related proteins (Rab-1A, 2A, 3B, 6A, 6B, and 11A), and tubulins (α-8, α-chain-like 3, β-1, and β-6) were exclusively found in tubulin-rich MAP preparations. On the other hand, COP signalosome complex subunits (3, 4, 5, 6, 7A, and 8), eukaryotic translation initiation factors (2 subunit 2, 2 subunit 3, 3 subunit F, 3 subunit K, and 5A-2), proteasomal proteins (α-type-1, 2, and 4, β-type 1, 2, 4, 6, and 7), and vacuolar proteins (Vacuolar ATP synthase subunit B, brain isoform, vacuolar protein sorting-associated protein 26A, 29, 35, and 45, vacuolar proton pump subunit C 1 and D, vacuolar-sorting protein SNF8) were only found in tubulin-depleted MAPs (Supplementary table 9). Furthermore, tubulins were reduced by a factor of 2.0–3.7 comparing the Mascot scores of the same proteins derived from tubulin-rich and tubulin-depleted MAPs. This roughly indicates the reduction of tubulin in the tubulin-depleted preparation (Supplementary table 9).

The classification of the identified proteins according to published literature and Swiss-Prot entries considering gene ontologies and comments revealed the following major groups of non-brain specific proteins: 142 enzymes, 54 MT-associated proteins, 44 actin and actin-related proteins, 27 proteasomal proteins, 25 proteins involved in translation, 24 ubiquitin-related proteins, 19 heat shock proteins, 17 tubulin and tubulin-modifying proteins, 14 endosomal proteins or endosomal trafficking, 13 small GTPases, 12 vacuolar proteins, 9 myosins or myosin-associated proteins, 9 vesicle proteins, 8 proteins involved in actin and tubulin folding, and 7 septins (Fig. 3). The enzymes consisted of 40 kinases and 10 phosphatases among others (Supplementary table 9). In addition, 62 brain-specific proteins were identified, thereof 9 MT-associated proteins, 7 actin-related proteins, and 14 vesicle-related proteins were found as major groups (Fig. 3). Almost all standard MAPs were identified confirming that MAPs were highly enriched. Moreover, comparison with the synaptic vesicle proteome revealed that 138 synaptic vesicle proteins were identified (Supplementary table 9).

Furthermore, we compared the MAP protein list against the human proteome in Uniprot using DAVID (Huang et al. 2009). DAVID consists of analytical tools to extract biological meaning from large gene and protein list (http://david.abcc.ncifcrf.gov/tools.jsp). The results of the functional annotation tools are shown in Supplementary tables 11–15 and include functional annotation clustering, gene ontology, protein domains, pathways, and functional categories. The terms were ordered by P-values to rank

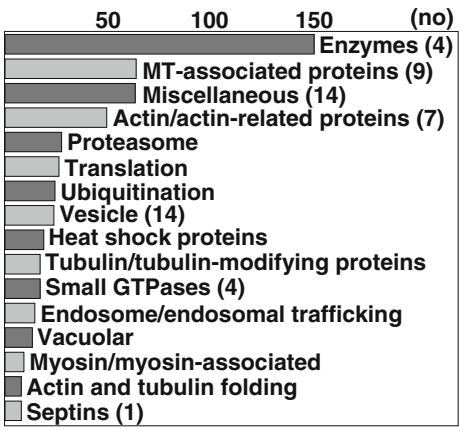

Fig. 3 Classification of found MAPs. The number of found MAPs according to protein classes is shown. The numbers of related brain-specific proteins are displayed as (*no*)

overall importance. Functional annotation clustering measures annotations terms on the basis of the degree of their co-association to cluster highly similar annotations into functional annotation groups (Huang et al. 2009). The most significant functional group comprehended the GO-terms cytoplasm/intracellular part/intracellular/cell part/cell, and the second most significant group included cytoskeleton/cytoskeletal part/cytoskeleton organization and biogenesis/microtubule/microtubule cytoskeleton/non-membrane-bound organelle/intracellular non-membrane-bound organelle/organelle organization and biogenesis/microtubule-based process/organelle part/intracellular organelle part/microtubule-based movement (Supplementary table 11), also confirming the enrichment of proteins of the cytoskeleton and microtubules. The top hit in protein domains and pathways has been the proteasome (Supplementary tables 13 and 14). The keywords nucleotide binding, microtubule, GTP-binding proteasome, cytoskeleton, actin-binding, and motor proteins have been in the top list with lowest P-values in functional categories (Supplementary table 15).

Posttranslational modifications of MAPs

The automatic error-tolerant search function in Mascot was applied to identify posttranslational modifications. The peptide matches with putative modifications were checked and well-known modifications produced by sample treatment and gel electrophoresis were excluded.

N-terminal protein acetylation is a well-known post-translational modification in eukaryotes. In total, 10 proteins were found to be N-terminally acetylated; thereof eight were identified with a mass difference of +42 Da as "Acetyl (Protein N-term)" and "Met-loss + Acetyl (Protein N-term)", one with a mass difference of +58 Da as "Acetyl (Protein N-term, oxidation (M)", and one with a mass difference of −89 Da as "Met-loss + Acetyl (Protein N-term)" (Table 1).

A mass shift of +4 Da can arise due to kynurenine formation of tryptophan or substitution of proline by threonine. However, the non-proline-containing peptide SEWSDLLSDLQK of 6-phosphofructokinase and the corresponding MS/MS spectra of the unmodified and modified peptide (Fig. 4a) confirmed kynurenine formation.

A mass shift of +48 Da can be justified by cysteine trioxidation, substitution of valine to phenylalanine or aspartic acid to tyrosine. The detected b- and y-ion series excluded valine and aspartic acid substitution, respectively, and confirmed cysteine trioxidation of the β-tubulin peptide EIVHLQAGQCGNQIGAK (Fig. 4b) and the MAP 1A/1B light chain 3A peptide SFADRCKEVQQIR (Fig. 4c).

A mass shift of +80 Da can occur due to phosphorylation at serine, threonine, tyrosine, or sulfonation at tyrosine. The peptides RETGVDLTK (75 kDa glucose-regulated protein), AEEAKDEPPSEGEAEEEEK and AEEAKDEPPSEGEAEEEEKK (Neurofilament light polypeptide), IYHLPDAESDEDEDFKEQTR (Septin-2), and DASPGRGSHSQTPSPGALPLGR (Synapsin-1) could be clearly assigned to be modified at a specific amino acid position due to the detected b- and y-ion series (Supplementary figures 1). Phosphorylation of tau (TAU_BOVIN) was identified at four sites (Supplementary table 1). Interestingly, the non-, mono-, and diphosphorylated peptides with one missed cleavage site and the corresponding mono-, di-, and triphosphorylated peptides with two missed cleavage sites were found. However, the monophosphorylated peptides were modified at another amino acid than the diphosphorylated peptides (Fig. 4d–f, Table 1, and Supplementary table 1).

To compare the efficiency of identifying phosphorylated peptides by the error-tolerant search, we also performed MS/MS analysis of tryptic digests from SDS-PAGE by enrichment using TiO_2 beads. Eleven phosphopeptides with a Mascot ion score >30 were identified in comparison to eight phosphopeptides found by the error-tolerant search (Table 1) in SwissProt. However, 50 phosphopeptides were found in addition by searching the data of phosphopeptide enrichment with TiO_2 beads at the NCBI (Table 1). Thereof, multiple phosphorylation sites were found for MAP 1A isoform 1 (gi 194676955) with 17 identified phosphopeptides, 19 phosphopeptides of MAP 1B isoform 2 (gi 76646182), and 12 phosphopeptides of MAP 2 isoform 1 (gi 76610296) (Table 1).

Sometimes certain mass differences can be attributed to distinct protein modifications. The mass change of +16 Da within the peptide ITQVDFPPR of cytoplasmic dynein 1 intermediate chain 2 was clearly observed at proline-7 by the MS/MS spectrum (Supplementary figures 1), but hydroxylation of proline cannot be distinguished by ion trap mass spectrometry from amino acid substitution of proline to leucine or isoleucine. The peptide ASLGHPATFGR (N(G),N(G)-dimethylarginine dimethylaminohydrolase 1) was found with a mass shift of +42 Da. According to Unimod the substitution of glycine to valine, acetylation of lysine or serine, and trimethylation of lysine can justify this mass difference. The matched b- and y-ions confirmed that either alanine-1 or serine-2 was modified. Although a change of alanine to isoleucine or leucine cannot be accounted by a single base substitution and thus was not obtained by Unimod, this cannot be fully excluded being responsible for the observed mass shift of +42 Da. Particularly, the peptide YIHSANVLHR (Mitogen-activated protein kinase 1) was also found with a mass shift of +42 Da and was assigned to being acetylated at serine-4

Table 1 List of peptides with posttranslational modifications, amino acid changes, and potential alternative splice variants

Accession	Sequence	*m*/*z* (*z*)	Δ*m*	PTM, AAE, ASV	Ion score
1433F_BOVIN	DNLTLWTSDQQDEEAGEGN	1,097.86 (2)	72+	G18: E	60 (47)
1433T_BOVIN	MEKTELIQK	581.31 (2)	42+	Acetyl (Prot. N-term)	37
1433Z_BOVIN	YLAEVAAGDDK	605.34 (3)	58+	A3: E	39
AP2A2_BOVIN	THIETVINALK	612.89 (2)	14−	E4: D	43
AP2A2_BOVIN	ILVAGDTMDSVK	617.82 (2)	14−	T7: S	65
AP2A2_BOVIN	FFQPTEMASQDFFQR	932.40 (2)	16−	S9: A	74
AP2A2_BOVIN	VIQIVINRDDYQGYYAAK	630.65 (3)	12−	I6: T	52
APOE_BOVIN	LHGRLEEVGVR	598.34 (2)	69−	R6: S	35
APOE_BOVIN	QKLHGRLEEVGVR	484.99 (3)	69−	R6: S	47
CLH1_BOVIN	QLLEKWLKEDK	707.82 (2)	15−	K5: I	40
COF1_BOVIN	ASGVAVSDGVIK	572.77 (2)	42+	Acetyl (Prot. N-term)	68
COF1_BOVIN	ASGVAVSDGVIK	580.80 (2)	16+	V6: D	37
DC1I2_BOVIN	ITQVDFPPR	544.93 (2)	16+	P7: L or hydroxylation	68 (58)
DC1I2_BOVIN	MSDKSELKAELER	482.98 (3)	42+	Met-loss + Acetyl	44
DDAH1_BOVIN	ASLGHPATFGR	578.39 (2)	42+	S2: Acetyl or A1: I/L	39
DNM1L_BOVIN	NAASGGGGVGDAVQEPTTGNWR	696.39 (3)	14−	E15: D or T18/19: S	41
GRP75_BOVIN	RETGVDLTK	549.60 (2)	80+	T3: Phosphorylation	44
GRP78_BOVIN	TFAPEEISAMVLTK	767.05 (2)	4−	T1: P	74
HSP7C_BOVIN	TTPSYVAFTDTER*	742.40 (2)	4−	T1/2: P	72
IF4H_BOVIN	MADFDTYDDRAYSSFGGGR	1,021.39 (2)	89−	Met-loss + Acetyl	42
K6PF_BOVIN	SEWSDLLSDLQK	712.81 (2)	4+	W3: Trp to Kynurenine	46 (72)
LASP1_BOVIN	TGDTGMLPANYVEAI	793.34 (2)	34+	I15: F	36 (34)
LASP1_BOVIN	TGDTGMLPANYVEAI	801.35 (2)	34+	I15: F	53 (56)
LDHB_BOVIN	SIAPVAEEETR	639.31 (2)	76+	S1: Y	36
MAP1S_BOVIN	AVLDALLAGK	514.80 (2)	58+	A8: E	62 (57)
MAP4_BOVIN	APATATLASPGSTSR	734.35 (2)	80+	S9: Phosphorylation	**57**
MARE1_BOVIN	ERDFYFGK	546.31 (2)	30+	G7: S	43
MARE1_BOVIN	LTVEDLEKER	580.33 (2)	72−	E4: G	42 (52)
MARE2_BOVIN	GERSYSWGMAVNVYSTSITQETMSR	914.92 (3)	99−	W7: S or R3: G	45
MK01_BOVIN	YIHSANVLHR	626.37 (2)	42+	S4: Acetyl or A5: I/L	38
MK01_BOVIN	AAAAAAGAGPEMVR	650.81 (2)	58+	Acetyl (Prot. N-term)	79
MLP3A_BOVIN	SFADRCKEVQQIR	543.65 (3)	48+	C6: Trioxidation	36
NCDN_BOVIN	MAALEQCLAEP	644.87 (2)	97+	QCLAE: Insertion of P	35
NFL_BOVIN	AAKDEVSESR	551.99 (2)	10+	S9: P	37
NFL_BOVIN	SSFSYEPYYSTSYKR	953.88 (2)	42+	Acetyl (Prot. N-term)	62
NFL_BOVIN	AEEAKDEPPSEGEAEEEEK	1,091.97 (2)	80+	S10: Phosphorylation	43
NFL_BOVIN	AEEAKDEPPSEGEAEEEEKEK	814.23 (3)	80+	S10: Phosphorylation	45
NFM_BOVIN	GVVTNGLDVSPGDEK	784.35 (2)	80+	S10: Phosphorylation	**105**
NFM_BOVIN	SYTLDSLGNPSAYR	793.41 (2)	42+	Acetyl (Prot. N-term)	74
NFM_BOVIN	GVVTNGLDVSPGDEKK	848.39 (2)	80+	S10: Phosphorylation	**76**
PHYIP_BOVIN	TEYSVAVQTAVK	646.32 (2)	4−	T1: P	33 (51)
RAB5C_BOVIN	QASPNIVIALAGNK	684.92 (2)	27−	N5: S	50
SBDS_BOVIN	SIFTPTNQIR	610.03 (2)	42+	Met-loss + Acetyl	37
SEPT2_BOVIN	IYHLPDAESDEDEDFKEQTR	839.74 (3)	80+	S9: Phosphorylation	50 **55**
STMN1_BOVIN	SKESVPEFPLSPPK	811.40 (2)	80+	S11: Phosphorylation	**43**
SYN1_BOVIN	DASPGRGSHSQTPSPGALPLGR	742.56 (3)	80+	S3: Phosphorylation	33
TAGL3_BOVIN	EVQEKIEQK	623.35 (2)	113+	QK: Insertion of I/L	34
TAU_BOVIN	KLDLSNVQSK	566.41 (2)		ASV: P29172-3/11/17	55

Table 1 continued

Accession	Sequence	*m*/*z* (*z*)	Δ*m*	PTM, AAE, ASV	Ion score
TAU_BOVIN	TPSLPTPPTR	573.78 (2)	80+	T6: Phosphorylation	**36**
TAU_BOVIN	SGYSSPGSPGTPGSR	777.28 (2)	160+	S4,8: Phosphorylation	**46**
TAU_BOVIN	VAVVRTPPKSPSAAK	530.24 (3)	80+	T6: Phosphorylation	48
TAU_BOVIN	HVPGGGSVQIVYKPVDLSK	990.66 (2)		ASV: P29172-3/11/17	55
TAU_BOVIN	TDHGAEIVYKSPVVSGDTSPR	765.80 (3)	80+	S19: Phosphorylation	45 (40) **63**
TAU_BOVIN	TDHGAEIVYKSPVVSGDTSPR	792.79 (3)	160+	S11,15: Phosphorylation	38 **39**
TAU_BOVIN	AKTDHGAEIVYKSPVVSGDTSPR	832.16 (3)	80+	S21: Phosphorylation	51
TAU_BOVIN	AKTDHGAEIVYKSPVVSGDTSPR	858.80 (3)	160+	S13,17: Phosphorylation	45 **39**
TAU_BOVIN	AKTDHGAEIVYKSPVVSGDTSPR	885.48 (3)	240+	S13,17,21: Phosphorylation	36 **55**
TAU_BOVIN	APAEIPEGTAAEEAGIGDTSNLED QAAGHVTQAR	1,126.64 (3)		ASV: P29172-02	56
TBA1D_BOVIN	IHFPLATYAPVISAEK	892.16 (2)	26+	H2: Y or I1:S	80 (69)
TBA1D_BOVIN	DVNAAIATIK	493.33 (2)	30−	T8: A	61 (75)
TBA1D_BOVIN	AVCMLSNTTAIAEAWAR**	895.43 (2)	18−	M4: I/L	92
TBA4A_BOVIN	LISQIVSSITASLR[#]	729.45 (2)	30−	S3: G	77
TBA8_BOVIN	HLFHPEQLITGKEDAANNYAR	800.12 (3)	26−	L2: S	61
TBB2B_BOVIN	EIVHLQAGQCGNQIGAK[##]	907.38 (2)	48+	C10: Trioxidation	51
TBB2B_BOVIN	LHFFMPGFAPLTSR[§]	824.18 (2)	26+	H2: Y	40 (52)
TBB2C_BOVIN	EEYPDRIMNTFSVVPSPK[§§]	670.90 (3)	99−	R6: G	42
TBB6_BOVIN	AALVDLEPGTTMDSVR	816.45 (2)	42+	A1 or A2: I/L	63
TCPG_BOVIN	ANITAIRR	430.25 (2)	55−	R7: T	37
TERA_BOVIN	ASGADSKGDDLSTAILG	845.92 (2)	42+	Met-loss + Acetyl	37
TPM3_BOVIN	MELQEIQLK	559.32 (2)	14−	Q7: N	39
TPPP_BOVIN	KGR.AGRVDLVDESGYYPGYK	684.98 (3)	227+	G-2: A	59
TPPP3_BOVIN	AASTDVAGLEESFRK	811.88 (2)	42+	Acetyl (Prot. N-term)	49
TRI17_BOVIN	LLQALKK	428.78 (2)	43+	L1: R	43
gi 194668168	SPPEPHTPPSTPVKLEEDLPR	801.2 (3)	80+	T7: Phosphorylation	**42**
gi 156120479	GILAADESTGSIAK	722.82 (2)	80+	S8: Phosphorylation	**51**
gi 194676955	ALGLEESPVQEDK	747.84 (2)	80+	S7: Phosphorylation	**32** (72)
gi 194676955	SPGSPPAQNPAEPLR	799.37 (2)	80+	S4: Phosphorylation	**45**
gi 194676955	GELSPSFLNPPLPR	802.40 (2)	80+	S4: Phosphorylation	**45**
gi 194676955	LPASSFSPTALLGEGR	841.91 (2)	80+	S7: Phosphorylation	**99**
gi 194676955	AATASPPTDGTSGYSAR	845.36 (2)	80+	S5: Phosphorylation	**44**
gi 194676955	LHTDLWPQGSPEDIR	922.42 (2)	80+	S10: Phosphorylation	**31**
gi 194676955	SPFEIISPPASPPEMAR	953.45 (2)	80+	S11: Phosphorylation	**36**
gi 194676955	SPFEIISPPASPPEMAR	1,001.43 (2)	160+	S7,11: Phosphorylation	**40**
gi 194676955	GFKSPPYEDFSVTGESEK	695.30 (3)	80+	S4: Phosphorylation	**61**
gi 194676955	QLSPESLGTLQFGELSLGK	1,042.52 (2)	80+	S3: Phosphorylation	**56**
gi 194676955	SLSLSEESPSKETSLDISSK	735.35 (3)	80+	S8: Phosphorylation	**58**
gi 194676955	GLSPEEAESLSVLSVVSPDAAK	1,133.05 (2)	80+	S3: Phosphorylation	**94**
gi 194676955	ELALSSPEDLTQDFEELKR	1,190.52 (2)	160+	S5,6: Phosphorylation	**31**
gi 194676955	QLSPESLGTLQFGELSLGKEEK	824.08 (3)	80+	S3: Phosphorylation	**44**
gi 194676955	SPGSPPAQNPAEPLREAGAVVAAAR	831.75 (3)	80+	S4: Phosphorylation	**44**
gi 76646182	SLMSSPEDLTK	652.28 (2)	80+	S5: Phosphorylation	**63**
gi 76646182	SLMSSPEDLTK	692.26 (2)	160+	S4,5: Phosphorylation	**32**
gi 76646182	SPSLSPSPPSPIEK	751.86 (2)	80+	S10: Phosphorylation	**33**
gi 76646182	TSKSPEDGGYAYEITEK	652.28 (3)	80+	S4: Phosphorylation	**69**
gi 76646182	AGATLEIKDTVSPVLDEK	656.00 (3)	80+	S12: Phosphorylation	**41**
gi 76646182	TTRSPEESGYAYEISEK	676.29 (3)	80+	S4: Phosphorylation	**58**

Table 1 continued

Accession	Sequence	*m/z* (*z*)	Δ*m*	PTM, AAE, ASV	Ion score
gi 76646182	ASISPMDEPVPDSESPIEK	1,062.46 (2)	80+	S15: Phosphorylation	**46** (80)
gi 76646182	HSLAEEEESAKAEADAHVK	533.49 (4)	80+	S2: Phosphorylation	**41**
gi 76646182	KLGGDVSPTQIDVSQFGSLK	719.36 (3)	80+	T9: Phosphorylation	**34**
gi 76646182	DYNASASTISPPSSMEEDKFSR	839.02 (3)	80+	S10: Phosphorylation	**39**
gi 76646182	DYNASASTISPPSSMEEDKFSR	865.67 (3)	160+	S10,13:Phosphorylation	**34**
gi 76646182	VSTSKHSLAEEEESAKAEADAHVK	659.06 (3)	80+	T3: Phosphorylation	**31**
gi 76646182	SLMSSPEDLTKDFEELKAEEVDVAK	969.45 (3)	80+	S5: Phosphorylation	**49**
gi 76646182	SEQSSMSIEFGQESPEHSLAMDFSR	976.73 (3)	80+	S14: Phosphorylation	**52** (71)
gi 76646182	SLMSSPEDLTKDFEELKAEEVDVAK	996.10 (3)	160+	S1,5: Phosphorylation	**38**
gi 76646182	ATVVVEAAEPEPSGSIANPAATTSPSLSHR	1,023.49 (3)	122+	Acetyl (Protein N-term); T23: Phosphorylation	**80**
gi 76646182	DTVSPVLDEKLSPPKSPSLSPSPPSPIEK	1,037.20 (3)	80+	S12: Phosphorylation	**54**
gi 76646182	QGVEDTEKFEDEGAGFEESSETGDYEEK	1,074.75 (3)	80+	S19: Phosphorylation	**31** (91)
gi 76646182	TDATDGRDYNASASTISPPSSMEEDKFSR	1,077.78 (3)	80+	S17: Phosphorylation	**48**
gi 76610296	VDHGAEIITQSPGR	780.36 (2)	80+	S11: Phosphorylation	**46**
gi 76610296	ARVDHGAEIITQSPGR	596.29 (3)	80+	S13: Phosphorylation	**45**
gi 76610296	ETSPESSLIQDEIAIK	920.44 (2)	80+	T2: Phosphorylation	**62** (70)
gi 76610296	KETSPESSLIQDEIAIK	984.48 (2)	80+	S4: Phosphorylation	**47**
gi 76610296	VKDEVSAEKEASPPISGDK	689.33 (3)	80+	S12: Phosphorylation	**46**
gi 76610296	KDEWGLVAPVSPGPLTPMK	706.68 (3)	80+	S11: Phosphorylation	**40**
gi 76610296	DGSPEAPASPEREEVGLSEYK	1,164.01 (2)	80+	S9: Phosphorylation	**42**
gi 76610296	DGSPEAPASPEREEVGLSEYK	1,203.99 (2)	160+	S3,9: Phosphorylation	**44**

The entry names of proteins identified with posttranslational modifications (PTM), amino acid exchanges (AAE), and alternative splice variants (ASV) are displayed. The peptide sequences identified by MS/MS, precursor masses (*m/z*) and charge (*z*), mass deviations calculated from the sequence database entry (Δ*m*), and peptide ion scores are shown. Position of AAEs, position and kind of PTMs, and accession number of ASVs are described. In addition, the ion scores of corresponding unchanged peptides are shown in parenthesis and phosphorylated peptides identified after enrichment with TiO_2 beads are displayed in bold. Identical peptide sequences were found for *HS71B_BOVIN, HSP72_BOVIN, **TBA4_BOVIN, TBA8_BOVIN, #TBA8_BOVIN, ##TBB2C_BOVIN TBB3_BOVIN, TBB4_BOVIN, §TBB5_BOVIN, and §§TBB4_BOVIN. More detailed information can be found in Supplementary table 10 and Mascot search results are shown in Supplementary figure 1

by Mascot. However, manual interpretation of the MS/MS spectrum allowing a substitution of alanine-5 to isoleucine or leucine also matched the intense mass peak at *m/z* 751.4 Da, which signified that an amino acid substitution was more likely than the acetylation of serine-4 (Supplementary figures 1). The peptide LLQALKK (Tripartite motif-containing protein) displayed a mass shift of +43 Da that can be explained either by carbamylation or an amino acid substitution of isoleucine or leucine to arginine. However, the complete y-ion series and b-ions indicated that leucine-1 was changed to arginine (Supplementary figures 1).

Amino acid insertions and exchanges of MAPs

Amino acid insertions were identified for two proteins (Table 1). The peptide EVQEKIEQK (Transgelin-3) displayed a mass difference of +113 Da, but no hit to this mass is displayed in Unimod. Considering the MS/MS spectrum with y-ions 2–6, the insertion of isoleucine or leucine, isobaric amino acids with the mass of 113 Da, must take place between glutamine-8 and lysine-9. Notably, this modification was only detected due to an assignment to a mass shift of +114 Da with a deviation of +1 Da, which was corrected to +113 Da. Another wrong assignment was observed for peptide MAALEQCLAEP (Neurochondrin) with a mass difference of +97 Da at cysteine-7 by maleimide, an unnatural modification. Considering the MS/MS spectrum, we justified a proline insertion between glutamine-6 and glutamic acid-10 for the mass shift.

Amino acid substitutions were observed for 34 peptides (Table 1). Only one amino acid substitution was possible for eight of the peptides (Supplementary table 1). The peptide AGRVDLVDESGYYPGYK (Tubulin polymerisation-promoting protein) matched with a mass difference

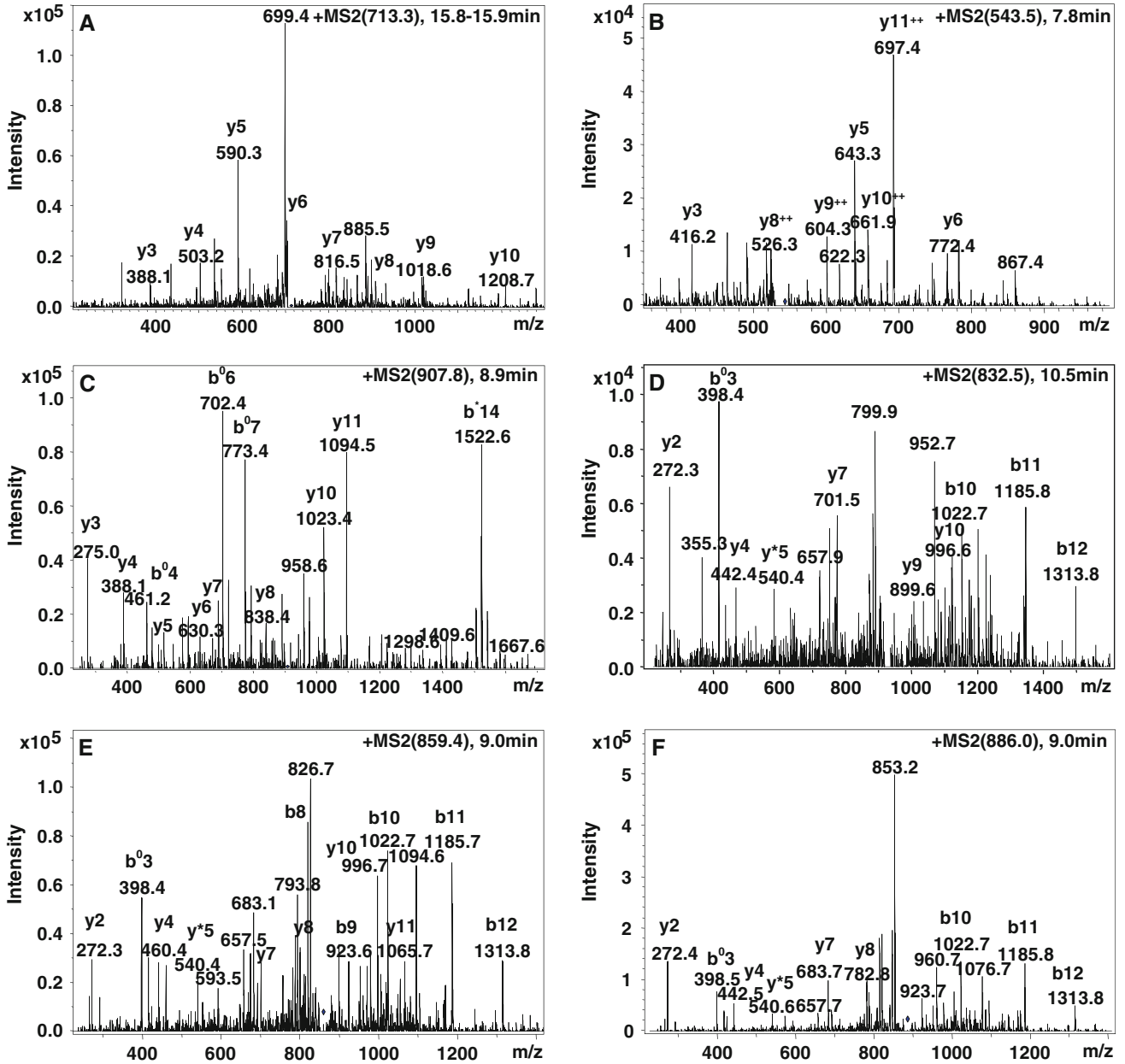

Fig. 4 MS/MS spectra of post-translationally modified tryptic peptides. The MS/MS spectrum with *m/z* 713.3 (**a**) was identified by a standard Mascot search as peptide SEWSDLLSDLQK with kynurenine modification and corresponded to 6-phosphofructokinase. The y-10 ion with *m/z* 1208.7 confirmed that the modification occurred at position 3. The MS/MS spectra with *m/z* 543.5 (**b**) and *m/z* 907.8 (**c**) were identified to be trioxidized at cysteines using the error-tolerant search function in Mascot. Thus, cysteine sulfonic acid modification was identified for MAP 1A/1B light chain 3A within the sequence SFADRCKEVQQIR (**b**), and for β-tubulin (**c**) within the sequence EIVHLQAGQCGNQIGAK. The MS/MS spectra with *m/z* 832.5 (**d**), *m/z* 859.4 (**e**), and *m/z* 886.0 (**f**) were identified as peptide AKTDHGAEIVYKSPVVSGDTSPR of tau with mono-, di-, and triphosphorylation. The MS/MS spectra showed that the monophosphorylated peptide was phosphorylated at serine-21, the diphosphorylated peptide at serines-13 and 17, and the triphosphorylated peptide at serines-13, 17, and 21

of +227 Da and could be explained by a missed cleavage site at the N-terminus, an alanine-to-glycine substitution (71 Da), and an additional arginine (156 Da) (Table 1). A single amino acid position for most of the amino acid substitutions could be attributed to the remaining 25 peptides (Supplementary table 10).

Alternative splice variants of MAPs

A Fasta database containing splice isoforms, variants, and conflicts described in Swiss-Prot annotations was generated for "other mammalia" because alternative splice variants of proteins can only be distinguished by mass spectrometry, if

Table 2 Overview of standard MAPs

MAPs classification	Protein name	Reference
Destabiliser	Kinesin-like protein KIF2A (Kinesin-2)	1
	Stathmin (Op18, prosolin, metablastin)	1
Linker	CAP-Gly domain-containing linker protein 1 (CLIP1)	1
	CLIP-associating protein 2 (CLAP2)	1
	Gephyrin	2
MT-based motor protein	Cytoplasmic dyneins & dynactin	1
	Kinesins	1
Severing	Katanin#	1
Stabiliser	MAP1 family	1
	Microtubule-associated protein 1A	
	Microtubule-associated protein 1B	
	Microtubule associated proteins 1A/1B light chain 3A*	
	Microtubule associated proteins 1A/1B light chain 3B	
	MAP RP/EB family	3–5
	Microtubule-associated protein RP/EB family member 1	
	Microtubule-associated protein RP/EB family member 2	
	Microtubule-associated protein RP/EB family member 3	
	WD repeat EMAP family	6
	Echinoderm microtubule-associated protein-like 1*	
	Echinoderm microtubule-associated protein-like 2*	
	Echinoderm microtubule-associated protein-like 3	
	Echinoderm microtubule-associated protein-like 4	
	Cytoskeleton-associated protein 5 (Dis1/Tog)	1
	Ferritin heavy chain (Syncolin)	1
	MAP7 domain-containing protein 1	1
	Microtubule-associated protein 2	1
	Microtubule-associated protein 4	1
	Microtubule-associated protein 7	1
	Microtubule-associated protein tau*	1
	STOP (MAP6)#	1
Other	AP-complex	1
	AP-1 complex subunit β-1	
	AP-2 complex subunit α-1	
	AP-2 complex subunit α-2*	
	AP-2 complex subunit β-1	
	AP-2 complex subunit σ-1	
	AP-3 complex subunit σ-1	
	Clathrin coat assembly protein AP180	1
	Mapmodulin#	1
	Mitotic checkpoint protein BUB3	1
	Phosphofurinacidic cluster sorting protein 1 (PACS1)	1

The proteins were classified according to Pollard and Earnshaw (2004). Unidentified proteins from bovine brain are marked with #. Proteins are indicated by an asterisk (*) for which additional posttranslational modifications, isoforms, or amino acid exchanges have been found. Table 3 includes detailed information about the MT-based motor proteins

Reference *1* Dutcher (2001), *2* Okajima et al. (1990), *3–5* Berrueta et al. (1998, 1999), Juwana et al. (1999), and *6* Eichenmuller et al. (2001)

the corresponding peptides were identified and the variants were included in the database. The datasets with the highest number of proteins and Mascot scores of tubulin-rich and tubulin-depleted MAPs were searched against this database. Currently, 20 tau isoforms are known to be generated by alternative splicing. We obtained splice form F as first hit

with an identical matching set of peptides for isoform Q, and matching subsets of these peptides for isoforms K, N, and, T. Deviating peptides of other isoforms with an ion score >30 were obtained for splice form C, and D with identical matching subsets of peptides for isoforms L, and R (Table 1 and Supplementary table 1).

Protein–protein interaction map

We retrieved binary interaction data for 549 of the 573 proteins listed in Supplementary table 9 using release 2.0 of the iRefIndex (see Razick et al. 2008 and http://irefindex.uio.no and methods). Figure 5 shows that 449 of these proteins plus a few (15) of their splice variants are present in one massive connected component while the majority of the remaining proteins (105) are singletons that do not interact with any other proteins in the seed list of 573 proteins. Protein nodes were colored according to their membership in one of four annotated groups of proteins according to Tables 1, 2, 3, and 4: standard MAPs (light blue), kinesin related (dark blue), actin related (red), and brain proteins (green). A total of 189 nodes were colored: 32 of these were single disconnected nodes while the majority were incorporated into the single connected component (152).

Discussion

MTs and their associated MAPs play essential roles in eukaryotic cells. Furthermore, their regulation is complex. Remarkably, many proteins, such as septins, have only recently been identified as MT/tubulin-binding proteins. Using bovine brain as the primary source for MAPs and their associated proteins, we identified a total of 573 proteins that associate with MTs. By applying two different purification procedures we showed that the number of identified MAPs depends on the biochemical preparation. For example, we were able to identify 114 unique proteins in tubulin-rich-, and 178 unique proteins in tubulin-depleted MAPs, resulting in a significantly increased number of proteins combining both preparations. In addition, in every cell type/tissue the fraction of MAPs might be different. As a consequence, different preparations from distinct tissues are likely to result in the identification of distinct classes of MAPs. For example, we identified a subgroup of about 60 brain-specific MAPs, which were not present in the MAP pools from the other three species previously investigated (*X. laevi, A. thaliana, D. melan*ogaster) (Chuong et al. 2004; Gache et al. 2007, 2010; Hughes et al. 2008; Liska et al. 2004). In addition, the MAPs identified from drosophila embryos (Hughes et al. 2008) represent a class of mitotic MT-associated proteins, absent in our study. We used endogenous bovine tubulin to purify MAPs from the same species. Previously, bovine tubulin was used to purify *X. laevis* and *A. thaliana* MAPs, which might result in a decreased affinity and explain the significantly increased number of MAPs identified with our approach. In addition, the sequence databases have increasing numbers of proteins identified in different organisms. For example, several proteins from the *A. thaliana* tubulin-binding proteins assigned as kinesin/dynein/myosin-like proteins (Chuong et al. 2004) are now identified in this study and assigned to the different motor protein super- and subfamilies. Due to the huge number of MAPs identified in our screen, we will concentrate in the following discussion mainly on important cytoskeleton-related and brain-specific protein groups.

"Conventional" MAPs

A prerequisite to construct proteome databases for MAPs is to verify that most of the identified proteins are essentially related to this subproteome. To validate our approach, we first searched for the presence of well-known "standard" MAPs (Pollard and Earnshaw 2004) (summarized in Table 2). Known mitotic MAPs could be excluded since no or extremely few proliferative cells are present in the adult brain (Eriksson et al. 1998). MAPs can be divided into six main classes such as MT destabilizers, severing proteins, stabilizers, linker proteins, motors and others. In total we identified almost all standard MAPs (Table 2), including many MT-based motor proteins, kinesins and dyneins, proteins involved in MT stabilization including four echinoderm MAP-like proteins, eleven MT-associated proteins, the linkers CLIP170 and CLASP2, and the destabilizers stathmin, and KIF2A. Thus, proteins of all main classes of MAPs were found with the exception of the severing protein katanin. STOP and mapmodulin have not been identified, but these proteins are not included in the Swiss-Prot database for bovine proteins and might not exist in bovine. In addition, we identified large, multisubunit complexes (e.g., AP-complex, dynein- and dynactin complexes, kinesin-adaptor-cargo complexes) and in particular MAP-associated proteins that interact but indirectly with MTs through association with one of the other MAPs. Astonishingly, in the two previous studies only very few standard MAPs have been identified, probably because exogenous tubulin was used for affinity purification of MAPs (Chuong et al. 2004; Hughes et al. 2008).

MT-based motor proteins and their associated proteins

Kinesins and dyneins form two superfamilies of motor proteins that are involved in intracellular transport. They play important roles in neuronal development (reviewed in Hirokawa and Noda 2008). In the brain, kinesins are

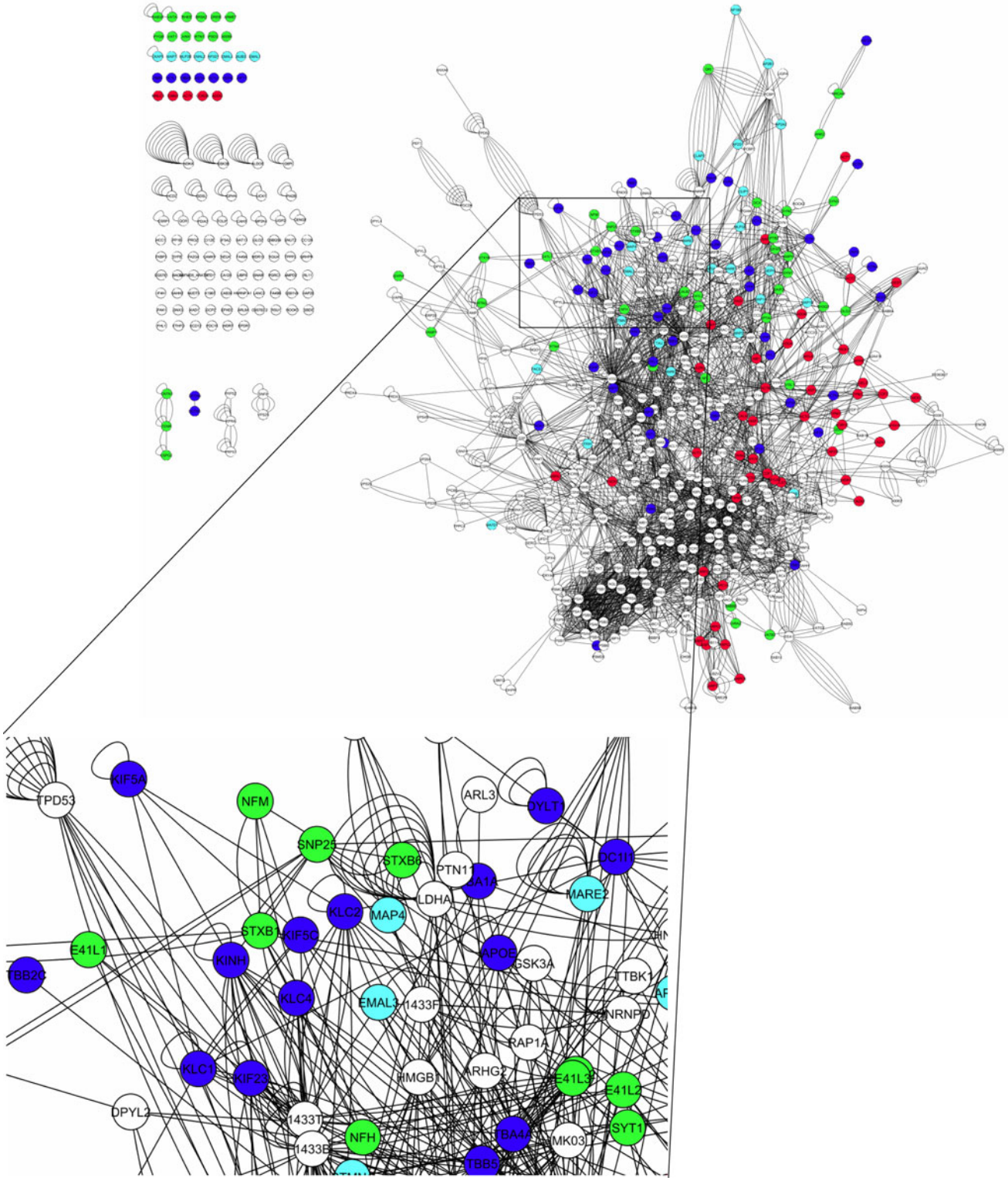

Fig. 5 Protein–protein interaction map. Protein–protein interaction data of the 573 identified proteins were retrieved using nine interaction databases. Interaction data were obtained for 549 proteins. Of these, 449 proteins were connected to a main cluster. 105 singletons and 10 proteins, which were not associated with the main cluster but interaction partners, are shown on the *left-hand side*. A part of the main cluster was magnified including several kinesins. Proteins were colored according to Tables 2, 3, 4, and 5 with *light blue* (standard MAPs), *dark blue* (MT-based motor proteins, kinesins and dyneins, the dynactin complex, and associated proteins), *red* (actins, myosins, the Arp2/3 complex, and associated proteins), and *green* (brain-specific proteins)

Table 3 Identified MT-based motor proteins, kinesins and dyneins, the dynactin complex, and associated proteins

Classification	Protein name	Reference
Dynactin complex	Dynactin subunits 1–6	1
	Actin, cytoplasmic 1	
	F-actin capping protein subunit α1, α2, β	
	α- and β-centractins	
Dynein	Cytoplasmic dynein heavy chain (DYHC)	2, 3
	Cytoplasmic dynein 1 intermediate chains 1 and 2	
	Cytoplasmic dynein 1 light intermediate chains 1 and 2	
	Cytoplasmic dynein light chains 1 and 2	
	Dynein light chain road block-type 1	
	Dynein light chain Tctex-type 1	
	Platelet-activating factor acetylhydrolase IB subunit α	
	Protein bicaudal D homolog 2	
Kinesin	Kinesin-like protein KIF2A	3, 4
Kinesin	Kinesin-like protein KIF21A	3, 5
Kinesin—KIF17	Kinesin-like protein KIF17	6
	Lin-7 homolog A (MALS)	
Kinesin—KIF23	Kinesin-like protein KIF23 (MKLP-1)	3, 7, 8
	Rac GTPase-activating protein 1 (MgcRacGAP)	
Kinesin—KIF5′s	Kinesin-like protein KIF5A, KIF5B (KINH), KIF5C	3, 9–15
	Kinesin light chain 1 (KLC1), 2 (KLC2), 4 (KLC4)	
	Apolipoprotein E	
	Cytoplasmic FMR1-interacting protein 2	
	Microtubule-associated protein tau	
	Myosins	
	Synaptosomal-associated protein 25	
	Syntaxin-1B	
	α-tubulins	
	β-tubulins	
	Vesicle-associated membrane protein 1 (Synaptobrevin-1)	
	RNA-transporting granule:	16
	Cytoplasmic FMR1-interacting protein 1	
	Elongation factor 1-α1	
	Eukaryotic translation initiation factors	
	Heterogeneous nuclear ribonucleoprotein A1	
	Hsp70	
	Transcriptional activator protein Pur-α	

Reference *1* Schroer (2004), *2* Hook and Vallee (2006), *3* Pollard and Earnshaw (2004), *4* Homma et al. (2003), *5* Berrueta et al. (1999), *6* Setou et al. (2000), *7* Sharp et al. (1997), *8* Mishima et al. (2002), *9–15* Diefenbach et al. (2002), Gyoeva et al. (2004), Huang et al. (1999), Kimura et al. (2005), Setou et al. (2002), Utton et al. (2005), Verhey et al. (2001), and *16* Kanai et al. (2004)

involved in directional axonal and dendritic transport of membrane organelles, protein complexes, and mRNAs along MTs. Cargo recognition occurs through scaffolding or adaptor protein complexes. Most kinesins are anterograde motors, moving to the plus end of MTs. We identified seven members (KIF2A, KIF5A, KIF5B, KIF5C, KIF17, KIF21A, and KIF23) of the kinesin superfamily and many of their associated proteins (Table 3), but as expected no mitotic kinesins. KIF2A, a MT depolymerising motor, suppresses collateral branch extension (Homma et al. 2003). The three members of the kinesin-1 family, KIF5A, KIF5B (conventional kinesin), and KIF5C, are the most abundant kinesins. While KIF5A and KIF5C are neuron-specific motors, KIF5B is ubiquitously expressed. KIF5 transports cargoes along MTs in both, axons and dendrites (Setou et al. 2002; Verhey et al. 2001). We have identified a large number of KIF5-associated proteins that bind either directly or indirectly, via the identified kinesin

Table 4 Identified actins, myosins, the Arp2/3 complex, and associated proteins

Classification	Protein name
Actin	Actins
Actin-associated	α-adducin, β-adducin, γ-adducin
	γ-aminobutyric acid receptor-associated protein-like 2
	Abl interactor 1
	Calmodulin
	Calponin-3
	α-Centractin, β-Centractin
	Chimeric POTE-actin protein
	Cofilin-1 and cofilin-2
	Coronin-1C, and coronin-2B
	Destrin
	Ezrin
	Fascin
	F-actin capping protein subunit α-1, α-2, β-1
	Gelsolin
	LIM and SH3 domain protein 1
	Myc box-dependent-interacting protein 1
	Nck-associated protein 1
	Plastin-3
	Profilin-2
	Radixin
	Tropomodulin-2
	Tropomyosin α-3 chain
	Tropomyosin-1 α chain
	WD repeat-containing protein 1
	Wiskott-Aldrich syndrome protein family member 1
Arp2/3 complex	Actin-like protein 2
	Actin-like protein 3
	Actin-related protein 2/3 complex subunit 1A
	Actin-related protein 2/3 complex subunit 2
	Actin-related protein 2/3 complex subunit 3
	Actin-related protein 2/3 complex subunit 4
	Actin-related protein 2/3 complex subunit 5
	Actin-related protein 2/3 complex subunit 5-like protein
Myosin	Myosin-10
	Myosin-9
	Myosin-Va
	Myosin-VI
Myosin-associated	Myosin light polypeptide 6
	Myosin light polypeptide 6B
	Myosin regulatory light chain 2, nonsarcomeric
	Tripartite motif-containing protein 2
	Tripartite motif-containing protein 3

light chains KLC1, KLC2, and KLC4 (Diefenbach et al. 2002; Gyoeva et al. 2004; Huang et al. 1999; Kimura et al. 2005; Utton et al. 2005): apolipoprotein E, synaptosomal-associated protein 25, syntaxin, cytoplasmic FMR1-interaction protein 1 and 2, VAMP1 (synaptobrevin-1), tubulins, myosins, and tau as shown in Table 3. The function of the three large superfamilies of motors, kinesin, dyneins, and myosins is closely coordinated. For example, it has been shown that myosins are transported to the cell periphery by KIF5A, either through a direct or indirect association with organelles (Huang et al. 1999). It was shown that KIF5 transports tubulin dimers, mediated by KLCs through slow axonal transport (Kimura et al. 2005). KIF5 transports mRNAs along MTs in RNA-transporting granules containing a large number (∼100) of proteins involved in RNA transport, protein synthesis, RNA helicases, heterogeneous nuclear ribonucleoproteins (hnRNPs), and RNA-associated proteins (Kanai et al. 2004). We identified 8 out of the 42 proteins from the RNA granule in our preparation. KIF17, a plus-end directed motor, transports cargo along MTs in the dendrites (Setou et al. 2000), whereas most other kinesins transport cargoes within the axons. KIF21A, a plus-end directed motor, is found throughout neurons (Kimura et al. 2005), but the cargo of KIF21A is still unknown. KIF23 (MKLP-1), a kinesin with dual function in intracellular transport and mitosis, transports MTs from the cell body to the developing dendrite (Sharp et al. 1997) but has also been shown to form the centralspindlin complex with MgcRacGAP, essential for completion of cytokinesis (Mishima et al. 2002). On the other hand, kinesins involved in anterograde axonal transport such as the monomeric motors KIF1A, KIF1Bα/KIF1Bβ, or KIF13B (kinesin-3 family) were not found, but their associated proteins synaptophysin, synaptotagmin, and Rab3A were identified. Furthermore, KIF3 (kinesin-2 family), and KIFC2 (kinesin-14 family) are missing, which might be due to their low abundance or their large molecular mass (>200 kDa).

The cytoplasmic multi-subunit protein complex dynein (a member of the AAA+ family of ATPases) is involved in retrograde intracellular transport (minus-end directed motor), mitosis and directed cell movement (Hook and Vallee 2006; Pollard and Earnshaw 2004). We identified the dynein heavy chain together with its accessory subunits, dynein intermediate- (IC), light intermediate- (LIC), light chains (LC), and some additional transiently bound partners, in total 11 proteins (Table 3). Moreover, we identified the dynactin complex, which is required for almost all cytoplasmic dynein-based activity in eukaryotes (Schroer 2004). Ten different subunits of the dynactin complex are known, nine of which were identified as

Table 5 Identified brain-specific proteins

Protein name	Association with MT, SV, or PPI data	Reference
α-internexin	SV-transient with SV membrane	1–3, 4
Amphiphysin	SV-transient with SV membrane MT-dynamin interaction	2, 3, 5
Ankyrin-2	PPI-main cluster	
Band 4.1-like protein 1, 2, and 3	MT-tubulin & NUMA interaction	6–8
BR serine/threonine-protein kinase 2	SV	9
Brain-specific angiogenesis inhibitor 1-associated protein 2	PPI-main cluster	
Calretinin	PPI-main cluster	
Contactin-1	SV-transient with SV membrane	1
Cytoplasmic FMR1-interacting protein 1, & 2	MT-KIF5 granule transport	10
Disks large homolog 3	PPI-main cluster	
Drebrin	PPI-singleton	
Endophilin-A1	PPI-main cluster	
Glial fibrially acidic protein	PPI-main cluster	
Glycogen phosphorylase	PPI-singleton	
GTP-binding protein Di-Ras2	SV	1
GTP-binding protein Rheb	MT-interaction through spastin	3, 11
Hyaluronan and proteoglycan link protein 2	PPI-no interaction	
Myelin basic protein (MBP)	SV-transient with SV membrane	12, 13
Myelin P2 protein	MT-tubulin/P2X2 interaction	14
Neurofilament medium polypeptide	MT-interaction with Tau	3, 15
	SV-transient with SV membrane	
Neurofilament triplet H protein (200 kDa)	SV-transient with SV membrane	3, 15
Neurofilament triplet L protein (68 kDa)	SV-transient with SV membrane	3, 15
Neuronal cell adhesion molecule	MT-interacts with MACF1	16
Neuronal migration protein double cortin	MT-binding	17
PH and SEC7 domain-containing protein 3	PPI-singleton	
Protein ARMET	PPI-singleton	
Protein quaking	MT-MAP1B interaction	18
RabGDP dissociation inhibitor α	SV-Rab interactions	11
Ras-related protein Rab3A	SV-established SV protein	1–3
Ras-related protein Rab6B	MT-transported by KIF20A	3, 19
	SV-putative novel SV protein	
Reticulon-1	MT-interaction through spastin SV-putative novel SV protein	1, 3, 20
Reticulon-3	SV-putative novel SVP	1, 3, 21
Reticulon-4	SV-putative novel SVP	3, 22
Septin-3	SV	21
SH3-containing GRB2-like protein 3-interacting protein 1	PPI-no interaction	
Spectrin α-chain	SV-transient with SV membrane	1, 23, 24
Spectrin β-chain	MT-interaction through syntabulin and KIF5B	1, 23, 24
	SV-transient with SV membrane	
Synapsin-1	SV-transient with SV membrane	2, 25, 26
Synapsin-2	SV-transient with SV membrane	1, 3, 27
Synapsin-3	MT-transported by KIF1A	1, 3, 27
	SV-transient with SV membrane	
Synaptic vesicle membrane protein VAT-1	SV-established SV protein	2
Synaptogyrin-1, and 3	SV-established SV protein	1
Synaptophysin	MT-transported by KIF1A	1–3
	SV-established protein	

Table 5 continued

Protein name	Association with MT, SV, or PPI data	Reference
Synaptosomal-associated protein 25	SV-established SV protein	1, 3, 28
Synaptotagmin-1	SV-established SV protein	2, 29
Syntaxin-1B	SV-established SV protein	2, 30–32
Syntaxin-binding protein 1	MT-tubulin & tau interaction	33, 34
	SV-interaction with SNAP25 & syntaxin	
Syntaxin-binding protein 6	SV-interaction with SNAP25 & syntaxin	35
Tenascin-R	PPI-main cluster	36
Vacuolar ATP synthase catalytic subunit A	SV-established SV protein	2
Vacuolar ATP synthase subunit B	SV-established SV protein	2
Versican core protein	PPI-main cluster	
Vesicle-associated membrane protein 1	SV-putative novel SV protein	36
Visinin-like protein 1 (VILIP)	PPI-main cluster	

An association with MTs, either direct or indirect through MAPs or as a synaptic vesicle (SV) proteome member, has been reported in the literature for 39 of the 54 identified brain-specific proteins. Of the remaining 15 proteins, nine proteins were found by bioinformatic analysis of protein–protein interactions (PPI) within the main cluster, four as singletons, and 2 revealed no interaction data. For convenience several brain-specific proteins (e.g., KIF5A, KIF5C, and some KIF5 interacting partners) have been classified in Table 3

Reference *1* Takamori et al. (2006), *2* Burre et al. (2006), *3* Burre and Volknandt (2007), *4* Green and Liem (1989), *5* Yoshida and Takei (2005), *6–8* Correas and Avila (1988), Hill et al. (1985), Ye et al. (1999); *9* Inoue et al. (2006), *10* Kanai et al. (2004), *11* Peter et al. (1994), *12* Saoudi et al. (1995), *13* Galiano et al. (2006), *14* Gendreau et al. (2003), *15* Yuan et al. (2000), *16* Nakayama et al. (2002), *17* Gleeson et al. (1999), *18* Luton (2005), *19* Echard et al. (1998), *20* Mannan et al. (2006), *21* Xue et al. (2004), *22* Mishima et al. (2002), *23* Ishikawa et al. (1983), *24* Kann and Fouquet (1993), *25* Baines and Bennett (1986), *26* Bennett and Baines (1992), *27* Ferreira et al. (1992), *28* Mishra et al. (2006), *29* Honda et al. (2002), *30* Itoh et al. (1999), *31* Su et al. (2004), *32* Cai et al. (2007), *33* Bhaskar et al. (2004), *34* Scales et al. (2002), *35* Vaughan et al. (1994), and *36* Nakata and Hirokawa (2003)

summarized in Table 3. In addition, known dynein/dynactin accessory components such as EB1, CLIP-170, spectrin, Rab6, Rab7, and Lis1, have also been identified. Dynein transports lysosomes, late and recycling endosomes and elements of the Golgi appratus and a more complete list of dynactin binding partners is only now emerging (for review see Schroer 2004).

Actin-associated proteins

Altogether, we identified 61 (10%) actin and actin-related proteins (Table 4). The list represents a snapshot of the known actin cytoskeleton including the ARP2/3 complex and the dynactin complex (10 identified subunits, listed in Table 3). MT and actin filament networks cooperate functionally during vesicle and organelle transport and many other processes. Several identified proteins are known to interact with both, the MT- and actin network (Rodriguez et al. 2003), including tau (Yu and Rasenick 2006), MAP2c (Roger et al. 2004), coronin 1C (Goode et al. 1999), synapsin 1A and 1B (Aubert-Foucher et al. 1990), neurocalcin (Ivings et al. 2002), MAP1S (Orban-Nemeth et al. 2005) and molecular motors such as dynein, the dynactin complex, "hetero" myosin-kinesin complexes, and the promiscuous myosin Va, which can travel along actin- and diffuse along MT-tracks (Goode et al. 1999). Most likely, these proteins interconnect MTs and actin filaments resulting in copurification of actin with MTs, together with its actin-binding proteins during the purification procedure. Probably, most of the actin-related proteins bind indirectly to MTs, through association with actin filaments, likely to be mediated by proteins that crosstalk with both filamentous structures.

Synaptic vesicle transport and brain-specific proteins

Synaptic vesicles (SVs) are organelles crucial for neurotransmission [comprehensively summarized in Takamori et al. (2006) and Burre and Volknandt (2007)]. The SV proteome, the complete inventory of integral and membrane-associated proteins responsible for the organelle function, has been studied intensely. The proteome has been roughly divided into three categories: "established synaptic vesicle proteins", "transiently associated synaptic vesicle proteins", and "putative novel synaptic vesicle proteins". Interestingly, members of all three motor protein families have been shown to transiently associate with SVs including kinesins (KIF5A/KIF5B), myosins (Va, VIIb) and the dynein/dynactin complex, linking SVs to the cytoskeleton/MT network (Burre et al. 2006; Burre and Volknandt 2007). In fact, SV transport has been shown to be mediated by kinesins (Hirokawa and Noda 2008). In total we identified more than 140 SV proteins from the three synaptic vesicle protein classes (see Supplementary material section table 9), corresponding to roughly 25% of all identified proteins.

Brain MAPs and their associated proteins have not been investigated previously with a systematic proteomics approach as described here. Not surprisingly, about 10% of all identified proteins (57 proteins) are classified as brain-specific proteins. Interestingly, for 80% of these (summarized in Table 5) the association with MTs can be explained by either belonging to the SV proteome (50%), or by direct or indirect binding to MTs (30%).

Multisubunit complexes

A striking feature, which is common for many of the 573 identified proteins, is that they are part of large protein families (heat shock protein families 20, 40, 70, 90, tubulin folding complex) or represent subunits of protein complexes. To our surprise, almost all proteins (in the case of complexes at least one protein subunit) could be clearly linked to the cytoskeleton showing interactions with either tubulin or MTs.

MT-binding proteins

Bioinformatic analysis of protein–protein interactions revealed that interactions of more than 75% of the identified proteins were associated with a main cluster (Fig. 5). Out of the remaining proteins, no interaction data were retrieved for 24 proteins but six of them were known to be MT-associated. Of the 105 singletons, 37 proteins were known to be associated with MTs, since they belong to Tables 1, 2, 3, and 4. In total, no interaction with MTs has been reported in the literature or in different protein–protein interaction databases for 86 proteins (15%). Most of these proteins were functionally ordered to "enzyme" and "miscellaneous" (Supplementary table 9). However, the proteins without interaction data are potential novel MT binding proteins.

Protein species

The term protein species was defined to describe the different chemical forms of a protein (Jungblut et al. 1996, 2008). Modification of proteins is an important cellular strategy that enables cells to react dynamically to intracellular or environmental changes. Posttranslational modifications and alternative splicing are among the best-known protein species, whereas amino acid exchanges have not yet been defined separately in the current nomenclature for protein species (Schluter et al. 2009). A prerequisite to identify protein modifications using mass spectrometry is to identify the modified peptide by fragmentation analysis and to map the modified amino acid. For this purpose, we applied an error-tolerant search using the mass search program Mascot to uninterpreted MS/MS spectra derived from tubulin-rich and tubulin-depleted MAPs. Modifications can be found searching uninterpreted MS/MS spectra with the Unimod database, semi-tryptic cleavage, and amino acid exchanges due to base substitutions. However, the results must be carefully verified. We identified many well-known artificial modifications arising from sample treatment. Finally, 68 modified peptides were identified (Table 1). Phosphorylation of serine or threonine, N-terminal acetylation, trioxidation of cysteine, and kynurenine formation of tryptophan could be unambiguously assigned as posttranslational modifications. N-terminal protein acetylation stabilizes proteins and is a common modification in eukaryotic proteins. Phosphorylation is one of the most important posttranslational modifications and plays an important role in signal transduction. The identified phosphorylation site of Grp75 was previously unknown in bovine and human, and the phosphorylation sites of septin-2, synapsin-1 and tau were only recorded in human. Enrichment of phosphorylated peptides using TiO_2 beads revealed in Swiss-Prot 11 instead of 8 phosphorylated peptides with five peptides in common. Only one of the additionally identified six phosphorylation sites using TiO_2 beads was experimentally known, four were non-experimentally qualified by similarity, and the phosphorylation site of MAP4 was completely unpredicted. However, 50 additional phosphorylated peptides were found in NCBI, most of these originate from three microtubule-associated proteins (MAP 1A isoform 1, MAP 1b isoform 2, MAP 2 isoform 1), which are known to be highly phosphorylated. Trioxidation of cysteine to form a sulfonic acid was detected in MAP 1A/1B light chain 3A and β-tubulin (Table 1). A biological role of the detected modified cysteine is likely, because oxidation of cysteine plays an important role in protein structure and function (Jacob et al. 2003). Kynurenine formation, a rarely determined protein modification, was identified for 6-phosphofructokinase. Oxidative stress can result in the modification of tryptophan to kynurenine and changes the stability of proteins (Okajima et al. 1990).

Interestingly, we identified many amino acid substitutions (Table 1). In some cases, the corresponding sequence according to Swiss-Prot was identified as well. The occurrence of different protein species due to amino acid exchanges can be attributed to individual variations and might be functionally or structurally relevant. Furthermore, two amino acid insertions were accidentally identified. One peptide matched to a modification in Unimod but displayed a mass error of 1 Da, most likely to a wrong assignment of the ^{13}C ions. The other peptide was modified by chemical modification of maleimide, which has an identical mass change as an additional proline. However, amino acid exchanges can be explained by single base substitutions, but amino acid insertions can only be attributed to three missing bases by DNA sequencing.

Multiple transcripts can be generated from a single mRNA precursor by alternative splicing and thus increase protein diversity. However, identification of alternative splice sites by mass spectrometry is challenging because the few peptides including the splice site must be identified. Furthermore, the alternative splice site must be recorded in the protein entry. For this purpose, we have generated a Swiss-Prot database including known alternative splice sites. Three peptides of splice variants of tau were identified. One peptide corresponded to only one of the 20 known splice variants, whereas the other two peptides were identical for three isoforms of tau. Notably, neuron-specific tau is of outstanding interest, because it plays an important role in Alzheimer's and other diseases (Wang and Liu 2008). In neurons, tau is associated with MTs and interacts with kinesin, influencing axonal transport. Furthermore, alternative splice variants and post-translational modifications of tau have been found to be important in neurodegenerative diseases, collectively known as tauopathies. Although it is a big challenge to identify specific modified peptides in a protein with 20 alternative splice variants and more than 50 known phosphorylation, we have been able to unambiguously identify four phosphorylation sites and two splice variants of tau.

More than 100 different proteins were identified specifically in each of the tubulin-rich and tubulin-depleted MAPs preparations. Notably, this affected some protein classes such as the echinoderm MAP-like proteins, kinesins, myosins, and Ras-related proteins, which were predominantly found in tubulin-rich preparations, whereas the COP signalosome complex subunits, several eukaryotic translation initiation factors, several proteasomal proteins, and vacuolar proteins were exclusively identified in tubulin-depleted MAPs. As a result, the combined results from both preparations revealed more comprehensive data for the MAPs database. Furthermore, more than 100 MS/MS spectra showed that different classes of protein species of MAPs occurred. Compared to previous studies on MAPs, we were able to significantly increase the inventory of identified proteins. Our list will be a rich and helpful resource to identify and verify new MAPs and in particular their associated proteins. Based on this resource it is now also possible to compare and identify differences in the two subfractions, the MAP proteome and the proteome of MAP-associated proteins, from healthy and sick brain tissue, such as neurodegenerative diseases.

References

Alfarano C, Andrade CE, Anthony K, Bahroos N, Bajec M, Bantoft K, Betel D, Bobechko B, Boutilier K, Burgess E, Buzadzija K, Cavero R, D'Abreo C, Donaldson I, Dorairajoo D, Dumontier MJ, Dumontier MR, Earles V, Farrall R, Feldman H, Garderman E, Gong Y, Gonzaga R, Grytsan V, Gryz E, Gu V, Haldorsen E, Halupa A, Haw R, Hrvojic A, Hurrell L, Isserlin R, Jack F, Juma F, Khan A, Kon T, Konopinsky S, Le V, Lee E, Ling S, Magidin M, Moniakis J, Montojo J, Moore S, Muskat B, Ng I, Paraiso JP, Parker B, Pintilie G, Pirone R, Salama JJ, Sgro S, Shan T, Shu Y, Siew J, Skinner D, Snyder K, Stasiuk R, Strumpf D, Tuekam B, Tao S, Wang Z, White M, Willis R, Wolting C, Wong S, Wrong A, Xin C, Yao R, Yates B, Zhang S, Zheng K, Pawson T, Ouellette BF, Hogue CW (2005) The Biomolecular Interaction Network Database and related tools 2005 update. Nucleic Acids Res 33:D418–D424

Ambudkar SV, Kimchi-Sarfaty C, Sauna ZE, Gottesman MM (2003) P-glycoprotein: from genomics to mechanism. Oncogene 22:7468–7485

Amos LA, Schlieper D (2005) Microtubules and maps. Adv Protein Chem 71:257–298

Aubert-Foucher E, Deleage G, Font B (1990) Do synapsin I and microtubule-associated proteins bind to a common site on polymerized tubulin? Biochem Int 22:821–827

Bader GD, Betel D, Hogue CW (2003) BIND: the Biomolecular Interaction Network Database. Nucleic Acids Res 31:248–250

Baines AJ, Bennett V (1986) Synapsin I is a microtubule-bundling protein. Nature 319:145–147

Barsnes H, Vizcaino JA, Eidhammer I, Martens L (2009) PRIDE Converter: making proteomics data-sharing easy. Nat Biotechnol 27:598–599

Bennett AF, Baines AJ (1992) Bundling of microtubules by synapsin 1. Characterization of bundling and interaction of distinct sites in synapsin 1 head and tail domains with different sites in tubulin. Eur J Biochem 206:783–792

Berrueta L, Kraeft SK, Tirnauer JS, Schuyler SC, Chen LB, Hill DE, Pellman D, Bierer BE (1998) The adenomatous polyposis coli-binding protein EB1 is associated with cytoplasmic and spindle microtubules. Proc Natl Acad Sci USA 95:10596–10601

Berrueta L, Tirnauer JS, Schuyler SC, Pellman D, Bierer BE (1999) The APC-associated protein EB1 associates with components of the dynactin complex and cytoplasmic dynein intermediate chain. Curr Biol 9:425–428

Bhaskar K, Shareef MM, Sharma VM, Shetty AP, Ramamohan Y, Pant HC, Raju TR, Shetty KT (2004) Co-purification and localization of Munc18-1 (p67) and Cdk5 with neuronal cytoskeletal proteins. Neurochem Int 44:35–44

Bhat KM, Setaluri V (2007) Microtubule-associated proteins as targets in cancer chemotherapy. Clin Cancer Res 13:2849–2854

Brown KR, Jurisica I (2005) Online predicted human interaction database. Bioinformatics 21:2076–2082

Burre J, Volknandt W (2007) The synaptic vesicle proteome. J Neurochem 101:1448–1462

Burre J, Beckhaus T, Schagger H, Corvey C, Hofmann S, Karas M, Zimmermann H, Volknandt W (2006) Analysis of the synaptic vesicle proteome using three gel-based protein separation techniques. Proteomics 6:6250–6262

Cai Q, Pan PY, Sheng ZH (2007) Syntabulin-kinesin-1 family member 5B-mediated axonal transport contributes to activity-dependent presynaptic assembly. J Neurosci 27:7284–7296

Candiano G, Bruschi M, Musante L, Santucci L, Ghiggeri GM, Carnemolla B, Orecchia P, Zardi L, Righetti PG (2004) Blue silver: a very sensitive colloidal Coomassie G-250 staining for proteome analysis. Electrophoresis 25:1327–1333

Chatr-aryamontri A, Ceol A, Palazzi LM, Nardelli G, Schneider MV, Castagnoli L, Cesareni G (2007) MINT: the Molecular INTeraction database. Nucleic Acids Res 35:D572–D574

Chuong SD, Good AG, Taylor GJ, Freeman MC, Moorhead GB, Muench DG (2004) Large-scale identification of tubulin-binding proteins provides insight on subcellular trafficking, metabolic

channeling, and signaling in plant cells. Mol Cell Proteomics 3:970–983
Correas I, Avila J (1988) Erythrocyte protein 4.1 associates with tubulin. Biochem J 255:217–221
Diefenbach RJ, Diefenbach E, Douglas MW, Cunningham AL (2002) The heavy chain of conventional kinesin interacts with the SNARE proteins SNAP25 and SNAP23. Biochemistry 41:14906–14915
Dutcher SK (2001) The tubulin fraternity: alpha to eta. Curr Opin Cell Biol 13:49–54
Echard A, Jollivet F, Martinez O, Lacapere JJ, Rousselet A, Janoueix-Lerosey I, Goud B (1998) Interaction of a golgi-associated kinesin-like protein with Rab6. Science 279:580–585
Eichenmuller B, Ahrens DP, Li Q, Suprenant KA (2001) Saturable binding of the echinoderm microtubule-associated protein (EMAP) on microtubules, but not filamentous actin or vimentin filaments. Cell Motil Cytoskeleton 50:161–172
Eriksson PS, Perfilieva E, Bjork-Eriksson T, Alborn AM, Nordborg C, Peterson DA, Gage FH (1998) Neurogenesis in the adult human hippocampus. Nat Med 4:1313–1317
Ferreira A, Niclas J, Vale RD, Banker G, Kosik KS (1992) Suppression of kinesin expression in cultured hippocampal neurons using antisense oligonucleotides. J Cell Biol 117:595–606
Gache V, Waridel P, Luche S, Shevchenko A, Popov AV (2007) Purification and mass spectrometry identification of microtubule-binding proteins from Xenopus egg extracts. Methods Mol Med 137:29–43
Gache V, Waridel P, Winter C, Juhem A, Schroeder M, Shevchenko A, Popov AV (2010) Xenopus meiotic microtubule-associated interactome. PLoS One 5:e9248
Galiano MR, Andrieux A, Deloulme JC, Bosc C, Schweitzer A, Job D, Hallak ME (2006) Myelin basic protein functions as a microtubule stabilizing protein in differentiated oligodendrocytes. J Neurosci Res 84:534–541
Gendreau S, Schirmer J, Schmalzing G (2003) Identification of a tubulin binding motif on the P2X2 receptor. J Chromatogr B Analyt Technol Biomed Life Sci 786:311–318
Gleeson JG, Lin PT, Flanagan LA, Walsh CA (1999) Doublecortin is a microtubule-associated protein and is expressed widely by migrating neurons. Neuron 23:257–271
Goode BL, Wong JJ, Butty AC, Peter M, McCormack AL, Yates JR, Drubin DG, Barnes G (1999) Coronin promotes the rapid assembly and cross-linking of actin filaments and may link the actin and microtubule cytoskeletons in yeast. J Cell Biol 144:83–98
Green LA, Liem RK (1989) Beta-internexin is a microtubule-associated protein identical to the 70-kDa heat-shock cognate protein and the clathrin uncoating ATPase. J Biol Chem 264:15210–15215
Guldener U, Munsterkotter M, Oesterheld M, Pagel P, Ruepp A, Mewes HW, Stumpflen V (2006) MPact: the MIPS protein interaction resource on yeast. Nucleic Acids Res 34:D436–D441
Gundersen GG, Cook TA (1999) Microtubules and signal transduction. Curr Opin Cell Biol 11:81–94
Gyoeva FK, Sarkisov DV, Khodjakov AL, Minin AA (2004) The tetrameric molecule of conventional kinesin contains identical light chains. Biochemistry 43:13525–13531
Hermjakob H, Fleischmann W, Apweiler R (1999) Swissknife—'lazy parsing' of SWISS-PROT entries. Bioinformatics 15:771–772
Hermjakob H, Montecchi-Palazzi L, Lewington C, Mudali S, Kerrien S, Orchard S, Vingron M, Roechert B, Roepstorff P, Valencia A, Margalit H, Armstrong J, Bairoch A, Cesareni G, Sherman D, Apweiler R (2004) IntAct: an open source molecular interaction database. Nucleic Acids Res 32:D452–D455
Hill AM, Cassoly R, Chetrite G, Pantaloni D (1985) High molecular weight microtubule-associated proteins from pig brain are immunologically related to human erythrocyte membrane proteins spectrin, ankyrin, proteins 4.1 and 4.2. Biol Cell 53:141–147
Hirokawa N, Noda Y (2008) Intracellular transport and kinesin superfamily proteins, KIFs: structure, function, and dynamics. Physiol Rev 88:1089–1118
Homma N, Takei Y, Tanaka Y, Nakata T, Terada S, Kikkawa M, Noda Y, Hirokawa N (2003) Kinesin superfamily protein 2A (KIF2A) functions in suppression of collateral branch extension. Cell 114:229–239
Honda A, Yamada M, Saisu H, Takahashi H, Mori KJ, Abe T (2002) Direct, Ca2+-dependent interaction between tubulin and synaptotagmin I: a possible mechanism for attaching synaptic vesicles to microtubules. J Biol Chem 277:20234–20242
Hook P, Vallee RB (2006) The dynein family at a glance. J Cell Sci 119:4369–4371
Huang JD, Brady ST, Richards BW, Stenolen D, Resau JH, Copeland NG, Jenkins NA (1999) Direct interaction of microtubule- and actin-based transport motors. Nature 397:267–270
Huang DW, Sherman BT, Lempicki RA (2009) Systematic and integrative analysis of large gene lists using DAVID bioinformatics resources. Nat Protoc 4:44–57
Hughes JR, Meireles AM, Fisher KH, Garcia A, Antrobus PR, Wainman A, Zitzmann N, Deane C, Ohkura H, Wakefield JG (2008) A microtubule interactome: complexes with roles in cell cycle and mitosis. PLoS Biol 6:e98
Inoue E, Mochida S, Takagi H, Higa S, Deguchi-Tawarada M, Takao-Rikitsu E, Inoue M, Yao I, Takeuchi K, Kitajima I, Setou M, Ohtsuka T, Takai Y (2006) SAD: a presynaptic kinase associated with synaptic vesicles and the active zone cytomatrix that regulates neurotransmitter release. Neuron 50:261–275
Ishikawa M, Murofushi H, Sakai H (1983) Bundling of microtubules in vitro by fodrin. J Biochem 94:1209–1217
Itoh TJ, Fujiwara T, Shibuya T, Akagawa K, Hotani H (1999) Inhibition of microtubule assembly by HPC-1/syntaxin 1A, an exocytosis relating protein. Cell Struct Funct 24:359–364
Ivings L, Pennington SR, Jenkins R, Weiss JL, Burgoyne RD (2002) Identification of Ca2+-dependent binding partners for the neuronal calcium sensor protein neurocalcin delta: interaction with actin, clathrin and tubulin. Biochem J 363:599–608
Jacob C, Giles GI, Giles NM, Sies H (2003) Sulfur and selenium: the role of oxidation state in protein structure and function. Angew Chem Int Ed Engl 42:4742–4758
Jordan MA, Wilson L (2004) Microtubules as a target for anticancer drugs. Nat Rev Cancer 4:253–265
Jungblut P, Thiede B, Zimny-Arndt U, Muller EC, Scheler C, Wittmann-Liebold B, Otto A (1996) Resolution power of two-dimensional electrophoresis and identification of proteins from gels. Electrophoresis 17:839–847
Jungblut PR, Holzhutter HG, Apweiler R, Schluter H (2008) The speciation of the proteome. Chem Cent J 2:16
Juwana JP, Henderikx P, Mischo A, Wadle A, Fadle N, Gerlach K, Arends JW, Hoogenboom H, Pfreundschuh M, Renner C (1999) EB/RP gene family encodes tubulin binding proteins. Int J Cancer 81:275–284
Kanai Y, Dohmae N, Hirokawa N (2004) Kinesin transports RNA: isolation and characterization of an RNA-transporting granule. Neuron 43:513–525
Kann ML, Fouquet JP (1993) Association of spectrin with manchette microtubules in mammalian spermatids. Biol Cell 77:311–313
Kavallaris M, Tait AS, Walsh BJ, He L, Horwitz SB, Norris MD, Haber M (2001) Multiple microtubule alterations are associated with Vinca alkaloid resistance in human leukemia cells. Cancer Res 61:5803–5809
Kerrien S, Alam-Faruque Y, Aranda B, Bancarz I, Bridge A, Derow C, Dimmer E, Feuermann M, Friedrichsen A, Huntley R, Kohler C,

Khadake J, Leroy C, Liban A, Lieftink C, Montecchi-Palazzi L, Orchard S, Risse J, Robbe K, Roechert B, Thorneycroft D, Zhang Y, Apweiler R, Hermjakob H (2007) IntAct—open source resource for molecular interaction data. Nucleic Acids Res 35:D561–D565

Kimura T, Watanabe H, Iwamatsu A, Kaibuchi K (2005) Tubulin and CRMP-2 complex is transported via Kinesin-1. J Neurochem 93:1371–1382

Laemmli UK (1970) Cleavage of structural proteins during the assembly of the head of bacteriophage T4. Nature 227:680–685

Liska AJ, Popov AV, Sunyaev S, Coughlin P, Habermann B, Shevchenko A, Bork P, Karsenti E, Shevchenko A (2004) Homology-based functional proteomics by mass spectrometry: application to the Xenopus microtubule-associated proteome. Proteomics 4:2707–2721

Luton F (2005) The role of EFA6, exchange factor for Arf6, for tight junction assembly, functions, and interaction with the actin cytoskeleton. Methods Enzymol 404:332–345

Maiato H, Sampaio P, Sunkel CE (2004) Microtubule-associated proteins and their essential roles during mitosis. Int Rev Cytol 241:53–153

Mannan AU, Boehm J, Sauter SM, Rauber A, Byrne PC, Neesen J, Engel W (2006) Spastin, the most commonly mutated protein in hereditary spastic paraplegia interacts with Reticulon 1 an endoplasmic reticulum protein. Neurogenetics 7:93–103

McKean PG, Vaughan S, Gull K (2001) The extended tubulin superfamily. J Cell Sci 114:2723–2733

Mishima M, Kaitna S, Glotzer M (2002) Central spindle assembly and cytokinesis require a kinesin-like protein/RhoGAP complex with microtubule bundling activity. Dev Cell 2:41–54

Mishra GR, Suresh M, Kumaran K, Kannabiran N, Suresh S, Bala P, Shivakumar K, Anuradha N, Reddy R, Raghavan TM, Menon S, Hanumanthu G, Gupta M, Upendran S, Gupta S, Mahesh M, Jacob B, Mathew P, Chatterjee P, Arun KS, Sharma S, Chandrika KN, Deshpande N, Palvankar K, Raghavnath R, Krishnakanth R, Karathia H, Rekha B, Nayak R, Vishnupriya G, Kumar HG, Nagini M, Kumar GS, Jose R, Deepthi P, Mohan SS, Gandhi TK, Harsha HC, Deshpande KS, Sarker M, Prasad TS, Pandey A (2006) Human protein reference database—2006 update. Nucleic Acids Res 34:D411–D414

Mollinedo F, Gajate C (2003) Microtubules, microtubule-interfering agents and apoptosis. Apoptosis 8:413–450

Moss DK, Lane JD (2006) Microtubules: forgotten players in the apoptotic execution phase. Trends Cell Biol 16:330–338

Nakata T, Hirokawa N (2003) Microtubules provide directional cues for polarized axonal transport through interaction with kinesin motor head. J Cell Biol 162:1045–1055

Nakayama M, Kikuno R, Ohara O (2002) Protein-protein interactions between large proteins: two-hybrid screening using a functionally classified library composed of long cDNAs. Genome Res 12:1773–1784

Okajima T, Kawata Y, Hamaguchi K (1990) Chemical modification of tryptophan residues and stability changes in proteins. Biochemistry 29:9168–9175

Orban-Nemeth Z, Simader H, Badurek S, Trancikova A, Propst F (2005) Microtubule-associated protein 1S, a short and ubiquitously expressed member of the microtubule-associated protein 1 family. J Biol Chem 280:2257–2265

Pagel P, Kovac S, Oesterheld M, Brauner B, Dunger-Kaltenbach I, Frishman G, Montrone C, Mark P, Stumpflen V, Mewes HW, Ruepp A, Frishman D (2005) The MIPS mammalian protein-protein interaction database. Bioinformatics 21:832–834

Peri S, Navarro JD, Amanchy R, Kristiansen TZ, Jonnalagadda CK, Surendranath V, Niranjan V, Muthusamy B, Gandhi TK, Gronborg M, Ibarrola N, Deshpande N, Shanker K, Shivashankar HN, Rashmi BP, Ramya MA, Zhao Z, Chandrika KN, Padma N, Harsha HC, Yatish AJ, Kavitha MP, Menezes M, Choudhury DR, Suresh S, Ghosh N, Saravana R, Chandran S, Krishna S, Joy M, Anand SK, Madavan V, Joseph A, Wong GW, Schiemann WP, Constantinescu SN, Huang L, Khosravi-Far R, Steen H, Tewari M, Ghaffari S, Blobe GC, Dang CV, Garcia JG, Pevsner J, Jensen ON, Roepstorff P, Deshpande KS, Chinnaiyan AM, Hamosh A, Chakravarti A, Pandey A (2003) Development of human protein reference database as an initial platform for approaching systems biology in humans. Genome Res 13:2363–2371

Perkins DN, Pappin DJ, Creasy DM, Cottrell JS (1999) Probability-based protein identification by searching sequence databases using mass spectrometry data. Electrophoresis 20:3551–3567

Peter F, Nuoffer C, Pind SN, Balch WE (1994) Guanine nucleotide dissociation inhibitor is essential for Rab1 function in budding from the endoplasmic reticulum and transport through the Golgi stack. J Cell Biol 126:1393–1406

Pollard TD, Earnshaw WC (2004) Cell biology. Elsevier, pp 589–593

Razick S, Magklaras G, Donaldson IM (2008) iRefIndex: a consolidated protein interaction database with provenance. BMC Bioinformatics 9:405

Rodriguez OC, Schaefer AW, Mandato CA, Forscher P, Bement WM, Waterman-Storer CM (2003) Conserved microtubule-actin interactions in cell movement and morphogenesis. Nat Cell Biol 5:599–609

Roger B, Al-Bassam J, Dehmelt L, Milligan RA, Halpain S (2004) MAP2c, but not tau, binds and bundles F-actin via its microtubule binding domain. Curr Biol 14:363–371

Salwinski L, Miller CS, Smith AJ, Pettit FK, Bowie JU, Eisenberg D (2004) The Database of Interacting Proteins: 2004 update. Nucleic Acids Res 32:D449–D451

Saoudi Y, Paintrand I, Multigner L, Job D (1995) Stabilization and bundling of subtilisin-treated microtubules induced by microtubule associated proteins. J Cell Sci 108(Pt 1):357–367

Scales SJ, Hesser BA, Masuda ES, Scheller RH (2002) Amisyn, a novel syntaxin-binding protein that may regulate SNARE complex assembly. J Biol Chem 277:28271–28279

Schluter H, Apweiler R, Holzhutter HG, Jungblut PR (2009) Finding one's way in proteomics: a protein species nomenclature. Chem Cent J 3:11

Schroer TA (2004) Dynactin. Annu Rev Cell Dev Biol 20:759–779

Setou M, Nakagawa T, Seog DH, Hirokawa N (2000) Kinesin superfamily motor protein KIF17 and mLin-10 in NMDA receptor-containing vesicle transport. Science 288:1796–1802

Setou M, Seog DH, Tanaka Y, Kanai Y, Takei Y, Kawagishi M, Hirokawa N (2002) Glutamate-receptor-interacting protein GRIP1 directly steers kinesin to dendrites. Nature 417:83–87

Shannon P, Markiel A, Ozier O, Baliga NS, Wang JT, Ramage D, Amin N, Schwikowski B, Ideker T (2003) Cytoscape: a software environment for integrated models of biomolecular interaction networks. Genome Res 13:2498–2504

Sharp DJ, Yu W, Ferhat L, Kuriyama R, Rueger DC, Baas PW (1997) Identification of a microtubule-associated motor protein essential for dendritic differentiation. J Cell Biol 138:833–843

Sharp DJ, Rogers GC, Scholey JM (2000) Microtubule motors in mitosis. Nature 407:41–47

Stark C, Breitkreutz BJ, Reguly T, Boucher L, Breitkreutz A, Tyers M (2006) BioGRID: a general repository for interaction datasets. Nucleic Acids Res 34:D535–D539

Su Q, Cai Q, Gerwin C, Smith CL, Sheng ZH (2004) Syntabulin is a microtubule-associated protein implicated in syntaxin transport in neurons. Nat Cell Biol 6:941–953

Takamori S, Holt M, Stenius K, Lemke EA, Gronborg M, Riedel D, Urlaub H, Schenck S, Brugger B, Ringler P, Muller SA, Rammner B, Grater F, Hub JS, De Groot BL, Mieskes G, Moriyama Y, Klingauf J, Grubmuller H, Heuser J, Wieland F,

Jahn R (2006) Molecular anatomy of a trafficking organelle. Cell 127:831–846

UniProt consortium (2008) The universal protein resource (UniProt). Nucleic Acids Res 36:D190–D195

Utton MA, Noble WJ, Hill JE, Anderton BH, Hanger DP (2005) Molecular motors implicated in the axonal transport of tau and alpha-synuclein. J Cell Sci 118:4645–4654

Vaughan L, Weber P, D'Alessandri L, Zisch AH, Winterhalter KH (1994) Tenascin-contactin/F11 interactions: a clue for a developmental role? Perspect Dev Neurobiol 2:43–52

Verhey KJ, Meyer D, Deehan R, Blenis J, Schnapp BJ, Rapoport TA, Margolis B (2001) Cargo of kinesin identified as JIP scaffolding proteins and associated signaling molecules. J Cell Biol 152:959–970

Wade RH (2007) Microtubules: an overview. Methods Mol Med 137:1–16

Wang JZ, Liu F (2008) Microtubule-associated protein tau in development, degeneration and protection of neurons. Prog Neurobiol 85:148–175

Wang JZ, Grundke-Iqbal I, Iqbal K (2007) Kinases and phosphatases and tau sites involved in Alzheimer neurofibrillary degeneration. Eur J Neurosci 25:59–68

Williams RC Jr, Lee JC (1982) Preparation of tubulin from brain. Methods Enzymol 85(Pt B):376–385

Xue J, Tsang CW, Gai WP, Malladi CS, Trimble WS, Rostas JA, Robinson PJ (2004) Septin 3 (G-septin) is a developmentally regulated phosphoprotein enriched in presynaptic nerve terminals. J Neurochem 91:579–590

Ye K, Compton DA, Lai MM, Walensky LD, Snyder SH (1999) Protein 4.1N binding to nuclear mitotic apparatus protein in PC12 cells mediates the antiproliferative actions of nerve growth factor. J Neurosci 19:10747–10756

Yoshida Y, Takei K (2005) Stimulation of dynamin GTPase activity by amphiphysin. Methods Enzymol 404:528–537

Yu JZ, Rasenick MM (2006) Tau associates with actin in differentiating PC12 cells. FASEB J 20:1452–1461

Yu LR, Zhu Z, Chan KC, Issaq HJ, Dimitrov DS, Veenstra TD (2007) Improved titanium dioxide enrichment of phosphopeptides from HeLa cells and high confident phosphopeptide identification by cross-validation of MS/MS and MS/MS/MS spectra. J Proteome Res 6:4150–4162

Yuan A, Mills RG, Chia CP, Bray JJ (2000) Tubulin and neurofilament proteins are transported differently in axons of chicken motoneurons. Cell Mol Neurobiol 20:623–632